PHYSICAL REVIEW D, VOLUME 70, 094008

Charmless $B \to PP$ decays and new physics effects in the minimal supergravity model

Zhenjun Xiao[1,*]
[1]Department of Physics, Nanjing Normal University, Nanjing, Jiangsu 210097, China, and CCAST (World Laboratory), P.O. Box 8730, Beijing 100080, China

Wenjuan Zou[2]
[2]Department of Physics, Nanjing Normal University, Nanjing, Jiangsu 210097, China
(Received 19 July 2004; published 5 November 2004)

By employing the QCD factorization approach, we calculate the new physics contributions to the branching radios of the two-body charmless $B \to PP$ decays in the framework of the minimal supergravity (mSUGRA) model. Within the considered parameter space, we find that (a) the supersymmetric (SUSY) corrections to the Wilson coefficients C_k $(k = 3 - 6)$ are very small and can be neglected safely, but the leading order SUSY contributions to $C_{7\gamma}(M_W)$ and $C_{8g}(M_W)$ can be rather large and even change the sign of the corresponding coefficients in the standard model; (b) the possible SUSY contributions to those penguin-dominated decays in mSUGRA model can be as large as 30%-50%; (c) for the well measured $B \to K\pi$ decays, the significant SUSY contributions play an important role in improving the consistency of the theoretical predictions with the data; (d) for $B \to K\eta'$ decays, the theoretical predictions of the corresponding branching ratios become consistent with the data within 1 standard deviation after the inclusion of the large SUSY contributions in the mSUGRA model.

DOI: 10.1103/PhysRevD.70.094008 PACS numbers: 13.25.Hw, 12.15.Ji, 12.60.Jv, 14.40.Nd

I. INTRODUCTION

As is well known, the precision measurements of the B meson system can provide an insight into very high energy scales via the indirect loop effects of the new physics beyond the standard model (SM) [1,2]. Although currently available data agree well with the SM predictions, we generally believe that the B-factories can at least detect the first signals of new physics if it is there.

Among the $B \to PP$ (P stands for the pseudoscalar light mesons) decay channels considered in this paper, twelve of them have been measured with good accuracy. And the data indeed show some deviations from the SM expectations:

(i) The $K\eta'$ puzzle, the observed $B \to K\eta'$ branching ratios [3–5] are much larger than the corresponding SM predictions, appeared several years ago, and there is still no convincing theoretical interpretation for this puzzle after intensive studies in the framework of SM [6] and the new physics models [7].

(ii) The $K\pi$ puzzle comes from the ratios R_c and R_n for the four well measured $B \to K\pi$ decay rates as defined in Ref. [8]. The SM prediction is $R_c = R_n$ by neglecting the small exchange- and annihilation-type amplitudes [8], while the present data [9] yields

$$R_c^{\rm exp} = \frac{2\Gamma(B^+ \to K^+\pi^0)}{\Gamma(B^+ \to K^0\pi^+)} = 1.15 \pm 0.13, \qquad (1)$$

$$R_n^{\rm exp} = \frac{\Gamma(B_d^0 \to K^+\pi^-)}{2\Gamma(B_d^0 \to K^0\pi^0)} = 0.78 \pm 0.10 \qquad (2)$$

A discrepancy of 2.8σ exists here.

(iii) For $B \to \pi^0\pi^0$ decay, the measured branching ratio $Br(B \to \pi^0\pi^0) = (1.9 \pm 0.5) \times 10^{-6}$ [4,5,9] is about 5 times larger than the SM prediction.

Although not convincing, these discrepancies together with the so-called ϕK_s anomaly [10] may be the first hints of new physics beyond the SM in B experiments [11,12].

Up to now, the possible new physics contributions to rare B meson decays have been studied extensively, for example, in the Technicolor models [13], the two-Higgs-doublet models [14,15] and the supersymmetric models [16–19]. Among the various new physics models, the supersymmetric models are indeed the most frequently studied models in searching for new physics in B meson system. The minimal supersymmetric standard model (MSSM) [20] is the general and most economical low-energy supersymmetric extension of the SM. But it is hard to make definite predictions for the physical observables in B meson decays since there are more than 100 free parameters that appeared in the MSSM. In order to find the possible signals or hints of new physics beyond the SM from the data, various scenarios of the MSSM are proposed by imposing different constraints on it [20]. The minimal supergravity (mSUGRA) model [21] seems to be a very simple constrained MSSM model, since it has only five free parameters $\tan\beta$, $m_{\frac{1}{2}}$, m_0, A_0, and $\mathrm{sgn}(\mu)$ at the high energy scale.

The previous works in the framework of the mSUGRA model focused on the semileptonic, leptonic, and radiative rare B decays. In Refs. [16–18,22], for example, the

*Electronic address: xiaozhenjun@pine.njnu.edu.cn

authors studied the rare decays $B \to X_s \gamma$, $B \to X_s l\bar{l}$, $B \to l^+ l^-$, and the $B^0 - \bar{B}^0$ mixing in the mSUGRA model, and found some constraints on the parameter space of this model.

For $B \to PP$ decays, they have been studied in the SM [23–29], the Technicolor models [13] and the two-Higgs-doublet models [14]. In Ref. [30], Mishima and Sanda calculated the supersymmetric effects on $B \to \phi k$ decays in the PQCD approach [29] and predicted the values of CP asymmetries with the inclusion of the supersymmetric contribution. In this paper, we calculate the supersymmetric contributions to the branching radios of the 21 $B \to PP$ decay modes in the mSUGRA model by employing the QCD factorization approach (QCD FA) [25–27]. The contributions from chirally enhanced power corrections and weak annihilations are also taken into account. We find that the branching ratios of some decay modes can be enhanced significantly, and these new contributions can help us to give a new physics interpretation for the so-called "$K\eta'$" puzzle.

This paper is organized as follows. In Sec. II, we give a brief review for the minimal supergravity model. In Sec. III, we calculate the new penguin diagrams induced by new particles and extract out the new physics parts of the Wilson coefficients in the mSUGRA model. The calculation of $B \to PP$ decays in QCD factorization approach is also discussed in this section. In Sec. IV, we present the numerical results of the branching ratios for the 21 $B \to PP$ decay modes in the SM and the mSUGRA model, and make phenomenological analysis for those well measured decay modes. The final section is the summary.

II. OUTLINE OF THE MSUGRA MODEL

In the MSSM, the most general superpotential compatible with gauge invariance, renormalizability and R-parity conserving is written as [20]:

$$\mathcal{W} = \varepsilon_{\alpha\beta}[f_{Uij} Q_i^\alpha H_2^\beta U_j + f_{Dij} H_1^\alpha Q_i^\beta D_j + f_{Eij} H_1^\alpha L_i^\beta E_j - \mu H_1^\alpha H_2^\beta] \tag{3}$$

where f_D, f_U, and f_E are Yukawa coupling constants for down-type, up-type quarks, and leptons, respectively. The suffixes $\alpha, \beta = 1, 2$ are SU(2) indices and $i, j = 1, 2, 3$ are generation indices, $\varepsilon_{\alpha\beta}$ is the antisymmetric tensor with $\varepsilon_{12} = 1$. In addition to the SUSY invariant terms, a set of terms which explicitly but softly break SUSY should be added to the supersymmetric Lagrangian. A general form of the soft SUSY-breaking terms is given as [20]:

$$\begin{aligned} -\mathcal{L}_{\rm soft} = {}& (m_Q^2)_{ij} \tilde{q}_{Li}^+ \tilde{q}_{Lj} + (m_U^2)_{ij} \tilde{u}_{Ri}^* \tilde{u}_{Rj} + (m_D^2)_{ij} \tilde{d}_{Ri}^* \tilde{d}_{Rj} + (m_L^2)_{ij} \tilde{l}_{Li}^+ \tilde{l}_{Lj} + (m_E^2)_{ij} \tilde{e}_{Ri}^* \tilde{e}_{Rj} + \Delta_1^2 h_1^+ h_1 + \Delta_2^2 h_2^+ h_2 \\ & + \varepsilon_{\alpha\beta}[A_{Uij} \tilde{q}_{Li}^\alpha h_2^\beta \tilde{u}_{Rj}^* + A_{Dij} h_1^\alpha \tilde{q}_{Li}^\beta \tilde{d}_{Rj}^* + A_{Eij} h_1^\alpha \tilde{l}_{Li}^\beta \tilde{e}_{Rj}^* + B\mu h_1^\alpha h_2^\beta] + \frac{1}{2} m_{\tilde{B}} \tilde{B} \tilde{B} + \frac{1}{2} m_{\tilde{W}} \tilde{W} \tilde{W} + \frac{1}{2} m_{\tilde{G}} \tilde{G} \tilde{G} + H.C. \end{aligned} \tag{4}$$

where $\tilde{q}_{Li}$, $\tilde{u}_{Ri}^*$, $\tilde{d}_{Ri}^*$, $\tilde{l}_{Li}$, $\tilde{e}_{Ri}^*$, and h_1 and h_2 are scalar components of chiral superfields Q_i, U_i, D_i, L_i, E_i, H_1, and H_2 respectively, and $\tilde{B}$, $\tilde{W}$, and $\tilde{G}$ are $U(1)_Y$, $SU(2)_L$, and $SU(3)_C$ gauge fermions. And the terms appearing in Eq. (4) are the mass terms for the scalar fermions, mass and bilinear terms for the Higgs bosons, trilinear coupling terms between sfermions and Higgs bosons, and mass terms for the gluinos, Winos and binos, respectively.

In the mSUGRA model, a set of assumptions are added to the MSSM. One underlying assumption is that SUSY-breaking occurs in a hidden sector which communicates with the visible sector only through gravitational interactions. The free parameters in the MSSM are assumed to obey a set of boundary conditions at the Plank or grand unified theory (GUT) scale:

$$\begin{gathered} \alpha_1 = \alpha_2 = \alpha_3 = \alpha_X, \\ (m_Q^2)_{ij} = (m_U^2)_{ij} = (m_D^2)_{ij} = (m_L^2)_{ij} = (m_E^2)_{ij} = (m_0^2)\delta_{ij}, \\ \Delta_1^2 = \Delta_2^2 = m_0^2, \qquad A_{Uij} = f_{Uij} A_0, \qquad A_{Dij} = f_{Dij} A_0, \\ A_{Eij} = f_{Eij} A_0, \qquad m_{\tilde{B}} = m_{\tilde{W}} = m_{\tilde{G}} = m_{1/2} \end{gathered} \tag{5}$$

where $\alpha_i = g_i^2/(4\pi)$, and g_i $(i = 1, 2, 3)$ denotes the coupling constant of the $U(1)_Y$, $SU(2)_L$, $SU(3)_C$ gauge group, respectively. The unification of them is verified according to the experimental results from LEP1 [31] and can be fixed at the Grand Unification Scale $M_{\rm GUT} \sim 2 \times 10^{16}$ Gev. Besides the three parameters $m_{1/2}$, m_0 and A_0, the supersymmetric sector is described at GUT scale by the bilinear coupling B and the supersymmetric Higgs(ino) mass parameter μ. However, one has to require the radiative electroweak symmetry-breaking (EWSB) takes place at the low-energy scale. The effective potential of neutral Higgs fields at the tree-level is given by (to be precise, one-loop corrections to the scalar potential have been included in the program we used later)

$$\begin{aligned} V_{\rm Higgs} = {}& m_1^2 |h_1^0|^2 + m_2^2 |h_2^0|^2 + m_3^2 (h_1^0 h_2^0 + H.C) \\ & + \frac{g_1^2 + g_2^2}{8} (|h_1^0|^2 - |h_2^0|^2)^2 \end{aligned} \tag{6}$$

where we have used the usual shorthand notation: $m_1^2 = (\mu^2 + \Delta_1^2)$, $m_2^2 = (\mu^2 + \Delta_2^2)$, $m_3^2 = B\mu$. The radiative EWSB condition is

$$\left\langle \frac{\partial V}{\partial h_1^0} \right\rangle = \left\langle \frac{\partial V}{\partial h_2^0} \right\rangle = 0 \tag{7}$$

where the value h_1^0, h_2^0 denotes the vacuum expectation values of the two neutral Higgs fields as $\langle h_1^0 \rangle = v \cos\beta$, $\langle h_2^0 \rangle = v \sin\beta$ with $v = 174$ Gev. From Eq. (7), we can determine the values of μ^2 and $B\mu$:

$$\mu^2 = \frac{1}{2}[\tan 2\beta(\Delta_2^2 \tan\beta - \Delta_1^2 \cot\beta) - M_Z^2],$$
$$B\mu = \frac{1}{2} \sin 2\beta[\Delta_1^2 + \Delta_2^2 + 2\mu^2] \tag{8}$$

Through Eq. (8) we can see the sign of μ is not determined. Therefore only four continuous free parameters and an unknown sign are left in the mSUGRA model. They are:

$$\tan\beta, m_{1/2}, m_0, A_0, \mathrm{sgn}(\mu) \tag{9}$$

In the mSUGRA model, all other parameters at the electroweak scale are then determined through the five free parameters by the GUT universality and the renormalization group equation (RGE) evolution. In this paper, we calculate the SUSY and Higgs particle spectrum through a Fortran code: SUSPECT version 2.1 [32]. The important features of this code include (a) the renormalization group evolution between low and high energy scales; (b) consistent implementation of radiative electroweak symmetry-breaking; and (c) calculation of the physical particle masses with radiative corrections. Using this code, we obtain the SUSY and Higgs particle masses, and the mixing angles of squarks at the electroweak scale. From these low-energy supersymmetric parameters, the mixing matrices Γ^U,Γ^D for the up-type and the down-type squarks, the mixing matrices U, V, N for charginos and neutralinos are determined. The explicit expressions of the two 6×6 mixing matrices Γ^U and Γ^D, two 2×2 matrices U and V, and a 4×4 matrix N can be found in Refs. [32–34].

III. THE BASIC THEORETICAL FRAMEWORK FOR $B \to PP$

In this section, we present the theoretical framework and the relevant formulas for calculating the exclusive nonleptonic decays of the $B^\pm$ and B^0 mesons into two light pseudoscalar mesons.

A. Effective Hamiltonian and relevant Wilson coefficients in SM

In the SM, if we take into account only the operators up to dimensions 6, and assume $m_b \gg m_s$, the effective Hamiltonian for the quark level three-body decay $b \to qq'\bar{q}'$ ($q \in \{d, s\}$, $q' \in \{u, d, s\}$) at the scale μ reads [35]

$$\begin{aligned}\mathcal{H}_{\mathrm{eff}} = \frac{G_F}{\sqrt{2}}\Big\{&\sum_{i=1}^{2} C_i(\mu)[V_{ub}V_{uq}^* O_i^u(\mu) + V_{cb}V_{cq}^* O_i^c(\mu)] \\ &- V_{tb}V_{tq}^* \sum_{j=3}^{10} C_j(\mu) O_j(\mu) \\ &- V_{tb}V_{tq}^*[C_{7\gamma}(\mu) O_{7\gamma}(\mu) + C_{8g}(\mu) O_{8g}(\mu)]\Big\}\end{aligned} \tag{10}$$

where $V_{pb}V_{pq}^*$ is the products of elements of the Cabbibo-Kabayashi-Maskawa (CKM) quark mixing matrix [36]. And the current-current ($O_{1,2}$), QCD penguin ($O_{3,4,5,6}$), electroweak penguin ($O_{7,8,9,10}$), electromagnetic and chromomagnetic dipole operators ($O_{7\gamma}$ and O_{8g}) can be written as [37]

$$O_1^u = (\bar{q}u)_{V-A}(\bar{u}b)_{V-A}, \quad O_2^u = (\bar{q}_\alpha u_\beta)_{V-A}(\bar{u}_\beta b_\alpha)_{V-A}, \quad O_1^c = (\bar{q}c)_{V-A}(\bar{c}b)_{V-A}, \quad O_2^c = (\bar{q}_\alpha c_\beta)_{V-A}(\bar{c}_\beta b_\alpha)_{V-A},$$
$$O_3 = (\bar{q}b)_{V-A}\sum_{q'}(\bar{q}'q')_{V-A}, \quad O_4 = (\bar{q}_\alpha b_\beta)_{V-A}\sum_{q'}(\bar{q}_\beta' q_\alpha')_{V-A}, \quad O_5 = (\bar{q}b)_{V-A}\sum_{q'}(\bar{q}'q')_{V+A},$$
$$O_6 = (\bar{q}_\alpha b_\beta)_{V-A}\sum_{q'}(\bar{q}_\beta' q_\alpha')_{V+A}, \quad O_7 = \frac{3}{2}(\bar{q}b)_{V-A}\sum_{q'} e_{q'}(\bar{q}'q')_{V+A}, \quad O_8 = \frac{3}{2}(\bar{q}_\alpha b_\beta)_{V-A}\sum_{q'} e_{q'}(\bar{q}_\beta' q_\alpha')_{V+A},$$
$$O_9 = \frac{3}{2}(\bar{q}b)_{V-A}\sum_{q'} e_{q'}(\bar{q}'q')_{V-A}, \quad O_{10} = \frac{3}{2}(\bar{q}_\alpha b_\beta)_{V-A}\sum_{q'} e_{q'}(\bar{q}_\beta' q_\alpha')_{V-A}, \quad O_{7\gamma} = \frac{e}{8\pi^2} m_b \bar{q}_\alpha \sigma^{\mu\nu}(1+\gamma_5) b_\alpha F_{\mu\nu},$$
$$O_{8g} = \frac{g}{8\pi^2} m_b \bar{q}_\alpha \sigma^{\mu\nu}(1+\gamma_5) T^a_{\alpha\beta} b_\beta G^a_{\mu\nu}, \tag{11}$$

where $T^a (a = 1, ..., 8)$ stands for $SU(3)_c$ generators, α and β are the $SU(3)_C$ color indices, and $V \pm A \equiv \gamma_\mu(1 \pm \gamma_5)$ by definition. The sum over q' runs over the quark fields that are active at the scale $\mu = \mathcal{O}(m_b)$, i.e., $q' \in \{u, d, s, c, b\}$.

To calculate the nonleptonic B meson decays at next-to-leading order (NLO) in α_s and to leading power in $\Lambda_{\mathrm{QCD}}/m_b$, we should determine the Wilson coefficient $C_i(M_W)$ through matching of the full theory onto the five-quark low-energy effective theory where the $W^\pm$

TABLE I. In the NDR scheme, the values of LO and NLO Wilson coefficients $C_i(\mu)$ for $\mu = m_b/2, m_b, 2m_b$. Input parameters being used are $\Lambda^{(5)}_{\overline{ms}} = 0.225$ Gev, $\sin^2\theta_W = 0.23$, $m_b = 4.62$ Gev, $m_t = 175$ Gev, $M_W = 80.4$ Gev, and $\alpha_{em} = 1/128$.

	$\mu = m_b/2$		$\mu = m_b$		$\mu = 2m_b$	
	LO	NLO	LO	NLO	LO	NLO
C_1	1.179	1.134	1.115	1.080	1.072	1.043
C_2	−0.370	−0.280	−0.255	−0.180	−0.171	−0.104
C_3	0.019	0.020	0.012	0.013	0.008	0.008
C_4	−0.037	−0.048	−0.027	−0.034	−0.018	−0.023
C_5	0.010	0.012	0.008	0.010	0.006	0.007
C_6	−0.050	−0.062	−0.033	−0.040	−0.021	−0.026
C_7/α_{em}	0.018	−0.008	0.028	0.007	0.046	0.030
C_8/α_{em}	0.055	0.055	0.035	0.035	0.023	0.023
C_9/α_{em}	−1.398	−1.420	−1.318	−1.337	−1.255	−1.270
C_{10}/α_{em}	0.415	0.395	0.286	0.273	0.191	0.183
$C_{7\gamma}$	−0.360	−0.334	−0.316	−0.307	−0.281	−0.282
C_{8g}	−0.167		−0.150		−0.136	

gauge boson, top quark and all SUSY particles heavier than M_W are integrated out, and run the Wilson coefficients down to the low-energy scale $\mu \sim O(m_b)$ by using the QCD renormalization group equations. In Table I, we simply present the numerical results of the LO and NLO Wilson coefficient in the NDR scheme in different scales. More detailed analytical expressions can be found, for example, in Refs. [35,37].

B. Wilson coefficients in the mSUGRA model

In the mSUGRA model, the new physics contributions to the rare decays will manifest themselves through two channels. One is the new contributions to the Wilson coefficients of the same operators involved in the SM calculation, the other is to the Wilson coefficients of the new operators such as operators with opposite chiralities. In the SM, the latter is absent because they are suppressed by the ratio m_s/m_b. In the mSUGRA model, they can also be neglected, as shown in Ref. [38]. Therefore we here use the same operator base as in the SM.

It is well known that there are no SUSY contributions to the Wilson coefficients at the tree-level. There are five kinds of contributions to the quark level decay process $b \to q q' \bar{q}'$ at one-loop level, depending on specific particles propagated in the loops:

(i) the gauge boson $W^\pm$ and up-type quarks u, c, t, which leads to the contributions in the SM;
(ii) the charged-Higgs boson $H^\pm$ and up-type quarks u, c, t;
(iii) the charginos $\tilde{\chi}^\pm_{1,2}$ and the scalar up-type quarks $\tilde{u}, \tilde{c}, \tilde{t}$;
(iv) the neutralinos $\tilde{\chi}^0_{1,2,3,4}$ and the down-type squarks $\tilde{d}, \tilde{s}, \tilde{b}$;
(v) the gauginos $\tilde{g}$ and the down-type squarks $\tilde{d}, \tilde{s}, \tilde{b}$.

The new physics contributions from those superparticle loops may induce too large flavor changing neutral currents (FCNCs). To escape from the so-called SUSY flavor problem, degeneracy of masses of squarks and sleptons among different generations has been assumed in the minimal SUGRA model.

In order to determine the new physics contributions to Wilson coefficients $C_i (i = 3, 4, 5, 6)$, $C_{7\gamma}$, and C_{8g} [we ignore the new physics contributions to $C_i (i = 7, 8, 9, 10)$ because they are suppressed by a factor of α_{em}/α_s]at the M_w scale, we need to calculate the Feynman diagrams appeared in Fig. 1. First, by employing conservation of the gluonic current, we can define the effective vertex of the $b \to qg$ penguin processes as in Ref. [39]:

$$\Gamma^a_\mu(q^2) = \frac{ig_s}{4\pi^2} \bar{u}_q(p_q) T^a V_\mu(q^2) u_b(p_b) \tag{12}$$

with

$$V_\mu(q^2) = (q^2 g_{\mu\nu} - q_\mu q_\nu)\gamma^\nu [F_{1L}(q^2) P_L + F_{1R}(q^2) P_R] + i\sigma_{\mu\nu} q^\nu [F_{2L}(q^2) P_L + F_{2R}(q^2) P_R] \tag{13}$$

where $F_1(q^2)$ and $F_2(q^2)$ are the electric and magnetic

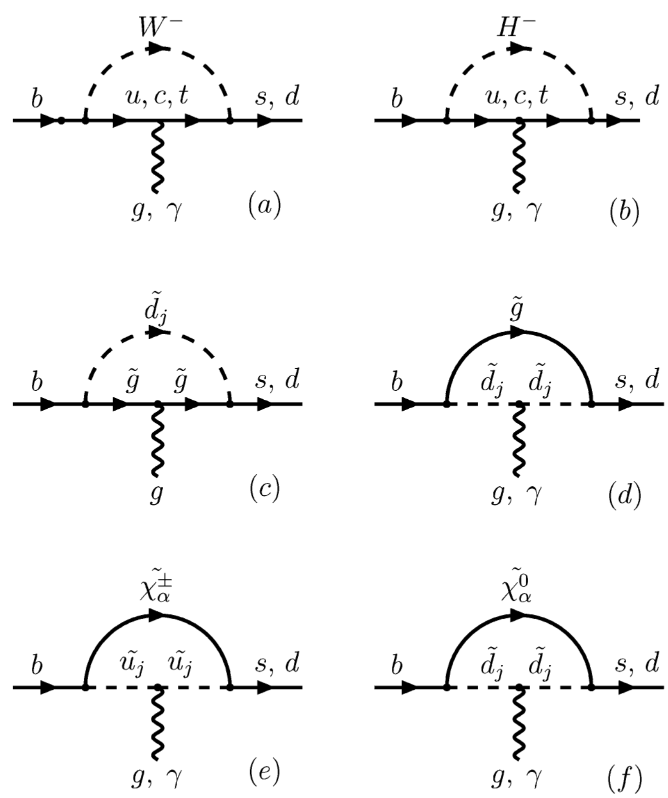

FIG. 1. Five kinds of loop contributions to $b \to qg, q\gamma$: (a) SM contribution. (b) charged-Higgs contribution; (c-d)- gluino contribution; (e) chargino contribution; (f) neutralino contribution.

form factors, $q = p_b - p_q$ is the gluon momentum, and $P_{L(R)} \equiv (1 \pm \gamma_5)/2$ are the chirality projection operators.

By calculating the Feynman diagrams as shown in Figs. 1(b)–1(f), we find [in the naive dimensional regularization (NDR) scheme,] the new physics parts of the Wilson coefficients at the scale M_W

$$C_k^{\rm NP}(M_W) = -\frac{\alpha_s(M_W)}{24\pi}\left[\frac{G_F}{\sqrt{2}}\lambda_t\right]^{-1} A_k F_{1L}(0) \qquad (14)$$

$$C_{8g}^{\rm NP}(M_W) = -\frac{F_{2R}(0)}{2}\left[\frac{G_F}{\sqrt{2}}\lambda_t m_b\right]^{-1} \qquad (15)$$

where $A_k \equiv \{-1, 3, -1, 3\}$ for $k = \{3, 4, 5, 6\}$, and $\lambda_t = V_{tq}^* V_{tb}$. In addition, since $q^2 \ll m_{\tilde{q}}^2$ where $m_{\tilde{q}}$ is the mass of the heavy scalar fermions, we set $q^2 = 0$ for the form factors $F_{1,2}$ as an approximation.[1] The explicit expressions of the form factors $F_{1L}(0)$ and $F_{2R}(0)$ induced by supersymmetric particles are the following

$$F_{1L}^{H^-}(0) = -\frac{G_F}{\sqrt{2}}\lambda_t x_{th}\cot^2\beta f_5(x_{th}), \qquad (16)$$

$$F_{2R}^{H^-}(0) = \frac{G_F}{\sqrt{2}}\lambda_t m_b x_{th}[\cot^2\beta f_1(x_{th}) + f_3(x_{th})], \qquad (17)$$

$$F_{1L}^{\tilde{g}}(0) = -\frac{g_s^2}{4m_{\tilde{g}}^2}\sum_{I=1}^{6}(\Gamma_{GL}^{d+})_j^I(\Gamma_{GL}^d)_I^3 f_6(x_{\tilde{d}_I\tilde{G}}), \qquad (18)$$

$$F_{2R}^{\tilde{g}}(0) = \sqrt{2}G_F\frac{g_s^2}{g^2}\sum_{I=1}^{6}x_{W\tilde{d}_I}(\Gamma_{GL}^{d+})_j^I\left\{(\Gamma_{GL}^d)_I^3 m_b\left[3f_1(x_{\tilde{G}\tilde{d}_I}) + \frac{1}{3}f_2(x_{\tilde{G}\tilde{d}_I})\right] + (\Gamma_{GL}^d)_I^3 m_{\tilde{G}}\left[3f_3(x_{\tilde{G}\tilde{d}_I}) + \frac{1}{3}f_4(x_{\tilde{G}\tilde{d}_I})\right]\right\}, \qquad (19)$$

$$F_{1L}^{\chi^-}(0) = -\frac{G_F}{\sqrt{2}}\sum_{\alpha=1}^{2}\sum_{I=1}^{6}x_{W\tilde{u}_I}(\Gamma_{CL}^{d+})_{\alpha j}^I(\Gamma_{CL}^d)_I^{\alpha 3}f_7(x_{\tilde{x}_\alpha^-\tilde{u}_I}), \qquad (20)$$

$$F_{2R}^{\chi^-}(0) = -\sqrt{2}G_F\sum_{\alpha=1}^{2}\sum_{I=1}^{6}x_{W\tilde{u}_I}(\Gamma_{CL}^{d+})_{\alpha j}^I \times[(\Gamma_{CL}^d)_I^{\alpha 3}m_b f_2(x_{\tilde{x}_\alpha^-\tilde{u}_I}) + (\Gamma_{CR}^d)_I^{\alpha 3}m_{\tilde{x}_\alpha^-}f_4(x_{\tilde{x}_\alpha^-\tilde{u}_I})], \qquad (21)$$

$$F_{1L}^{\chi^0}(0) = -\frac{G_F}{\sqrt{2}}\sum_{\alpha=1}^{4}\sum_{I=1}^{6}x_{W\tilde{d}_I}(\Gamma_{NL}^{d+})_{\alpha j}^I(\Gamma_{NL}^d)_I^{\alpha 3}f_7(x_{\tilde{x}_\alpha^0\tilde{d}_I}), \qquad (22)$$

$$F_{2R}^{\chi^0}(0) = -\sqrt{2}G_F\sum_{\alpha=1}^{4}\sum_{I=1}^{6}x_{W\tilde{d}_I}(\Gamma_{NL}^{d+})_{\alpha j}^I \times[(\Gamma_{NL}^d)_I^{\alpha 3}m_b f_2(x_{\tilde{x}_\alpha^0\tilde{d}_I}) + (\Gamma_{NR}^d)_I^{\alpha 3}m_{\tilde{x}_\alpha^0}f_4(x_{\tilde{x}_\alpha^0\tilde{d}_I})], \qquad (23)$$

where $j = 1$ for $b \to d$ and $j = 2$ for $b \to s$ decay, respectively. $x_{ij} = m_i^2/m_j^2$ and m_i is the mass of the particle i. In our calculations, we have set $m_q = 0$ for $q = u, d, s$ since $m_b \gg m_u, m_d$ and m_s. The one-loop integration functions $f_i(x)$ and the coupling constants $\Gamma_{G(L,R)}^d, \Gamma_{C(L,R)}^d, \Gamma_{N(L,R)}^d$ which appear in F_{1L} and F_{2R} are listed in the appendix. Using the form factors in Eqs. (16)–(23), we obtain the analytic expressions for $C_k^{\rm NP}(M_W)$ and $C_{8g}^{\rm NP}(M_W)$. The Wilson coefficient $C_{8g}^{\rm NP}(M_W)$ as given in Eq. (15) is the same as that in Ref. [18] except for some differences in expression. In Ref. [18], the CKM factor $-\lambda_t$ has not been extracted from Wilson coefficients, and the CKM matrix elements have been absorbed into the definition of the coupling constant Γ_L^U. See the appendix for more details.

For the effective vertex of the supersymmetric $b \to q\gamma$ penguin processes, we only consider its contributions to $C_{7\gamma}$. The explicit analytical expressions of the SUSY contribution to $C_{7\gamma}$ induced by new particles have been given in Ref. [18]

$$C_{7\gamma}^{H^-}(m_W) = -\frac{1}{2}x_{th}\left\{\cot^2\beta\left[\frac{2}{3}f_1(x_{th}) + f_2(x_{th})\right] + \left[\frac{2}{3}f_3(x_{th}) + f_4(x_{th})\right]\right\} \qquad (24)$$

$$C_{7\gamma}^{\tilde{g}}(m_W) = -\frac{8}{9}\frac{g_s^2}{g^2\lambda_t}\sum_{I=1}^{6}x_{W\tilde{d}_I}(\Gamma_{GL}^{d+})_j^I\left[(\Gamma_{GL}^d)_I^3 f_2(x_{\tilde{G}\tilde{d}_I}) + (\Gamma_{GR}^d)_I^3\frac{m_{\tilde{G}}}{m_b}f_4(x_{\tilde{G}\tilde{d}_I})\right] \qquad (25)$$

$$C_{7\gamma}^{\tilde{\chi}^-}(m_W) = \frac{1}{\lambda_t}\sum_{\alpha=1}^{2}\sum_{I=1}^{6}x_{W\tilde{u}_I}(\Gamma_{CL}^{d+})_{\alpha j}^I\left\{(\Gamma_{CL}^d)_I^{\alpha 3}\left[f_1(x_{\tilde{x}_\alpha^-\tilde{u}_I}) + \frac{2}{3}f_2(x_{\tilde{x}_\alpha^-\tilde{u}_I})\right] + (\Gamma_{CR}^d)_I^{\alpha 3}\frac{m_{\tilde{x}_\alpha^-}}{m_b}\left[f_3(x_{\tilde{x}_\alpha^-\tilde{u}_I}) + \frac{2}{3}f_4(x_{\tilde{x}_\alpha^-\tilde{u}_I})\right]\right\} \qquad (26)$$

$$C_{7\gamma}^{\tilde{\chi}^0}(m_W) = -\frac{1}{3\lambda_t}\sum_{\alpha=1}^{4}\sum_{I=1}^{6}x_{W\tilde{d}_I}(\Gamma_{NL}^{d+})_{\alpha j}^I\left[(\Gamma_{NL}^d)_I^{\alpha 3}f_2(x_{\tilde{x}_\alpha^0\tilde{d}_I}) + (\Gamma_{NR}^d)_I^{\alpha 3}\frac{m_{\tilde{x}_\alpha^0}}{m_b}f_4(x_{\tilde{x}_\alpha^0\tilde{d}_I})\right]. \qquad (27)$$

[1] Equations (14) and (15) differ from those appeared in Ref. [40], but our final analytic expressions for $C_{8g}^{\rm NP}(M_W)$ are the same as that in Ref. [18] except for the definition for Wilson coefficients.

Now, we found all the supersymmetric contributions to the relevant Wilson coefficients. We should remember that, the only source of flavor violation in the mSUGRA model is the usual CKM matrix in the SM. The flavor violation in the sfermion sector at the electroweak scale is generated radiatively in the mSUGRA model and consequently small. Therefore, if we take the mixing matrices Γ^U and Γ^D as given in the Appendix of Ref. [33]

$$\Gamma^U = \begin{bmatrix} 1 & 0 & 0 & 0 & 0 & 0 \\ 0 & 1 & 0 & 0 & 0 & 0 \\ 0 & 0 & \cos\theta_{\tilde{t}} & 0 & 0 & \sin\theta_{\tilde{t}} \\ 0 & 0 & 0 & 1 & 0 & 0 \\ 0 & 0 & 0 & 0 & 1 & 0 \\ 0 & 0 & -\sin\theta_{\tilde{t}} & 0 & 0 & \cos\theta_{\tilde{t}} \end{bmatrix}, \quad \Gamma^D = \begin{bmatrix} 1 & 0 & 0 & 0 & 0 & 0 \\ 0 & 1 & 0 & 0 & 0 & 0 \\ 0 & 0 & \cos\theta_{\tilde{b}} & 0 & 0 & \sin\theta_{\tilde{b}} \\ 0 & 0 & 0 & 1 & 0 & 0 \\ 0 & 0 & 0 & 0 & 1 & 0 \\ 0 & 0 & -\sin\theta_{\tilde{b}} & 0 & 0 & \cos\theta_{\tilde{b}} \end{bmatrix} \tag{28}$$

the gluino- and neutralino-mediated diagrams will not contribute to the decay processes considered here. The new physics contributions will come from the charged-Higgs and chargino diagrams only.

C. $B \to PP$ decays in QCD factorization

To calculate the decay amplitude of the processes $B \to PP$, the last but most important step is to calculate hadronic matrix elements for the hadronization of the final-state quarks into particular final states. At the present time, many approaches have been put forward to settle the intractable problem. Such as the native factorization [41], the generalized factorization [23,24], the QCD FA [25–27] and the PQCD approach [29]. In this paper, we employ the QCD FA to calculate the branching ratios of $B \to PP$ decays.

In QCD FA, the contribution of the nonperturbative sector is dominated in the form factors of $B \to P$ transition and the nonfactorizable impact in the hadronic matrix elements is controlled by hard gluon exchange. In the heavy quark limit $m_b \gg \Lambda_{\rm QCD}$ and to leading power in Λ_{QCD}/m_b, the hadronic matrix elements of the exclusive nonleptonic decays of the B meson into two light pseudoscalar mesons P_1, P_2 (P_1 absorbs the spectator quark coming from the B meson) can be written as [25]

$$\langle P_1P_2|O_i|B\rangle = \sum_j F_j^{B\to P_1} \int_0^1 dx T_{ij}^I(x)\Phi_{P_2}(x) + (P_1 \leftrightarrow P_2) + \int_0^1 d\xi \int_0^1 dx \int_0^1 dy T_i^{II}(\xi, x, y) \times \Phi_B(\xi)\Phi_{P_1}(x)\Phi_{P_2}(y) \tag{29}$$

where $F_j^{B\to P_1}$ is the form factor describing $B \to P_1$ decays. T_{ij}^I and T_i^{II} denote the perturbative short-distance interactions and can be calculated by the perturbation approach. $\Phi_X(x)(X = B, P_{1,2})$ are the universal and nonperturbative light cone distribution amplitudes (LCDA) for B and $P_{1,2}$ meson respectively [26]. Weak annihilation effects are not included in Eq. (29).

Consider the low-energy effective Hamiltonian Eq. (10) and the unitary relation of the CKM matrix, the decay amplitude can be written as

$$\mathcal{A}\,(B \to P_1P_2) = \frac{G_F}{\sqrt{2}} \sum_{p=u,c} \sum_i V_{pb}V_{pq}^* C_i(\mu)\langle P_1P_2|O_i|B\rangle \tag{30}$$

the effective hadronic matrix elements $\langle P_1P_2|O_i|B\rangle$ can be calculated by employing the QCD factorization formula Eq. (29). When considering order α_s corrections to the hard-scattering kernels T_{ij}^I and T_i^{II} from nonfactorizable single gluon exchange vertex correction diagrams, penguin diagrams and hard spectator scattering diagrams, and the contributions from the chirally enhanced power corrections,[2] Eq. (30) can be rewritten as [28]

$$\mathcal{A}^f(B \to P_1P_2) = \frac{G_F}{\sqrt{2}} \sum_{p=u,c} \sum_i V_{pb}V_{pq}^* a_i^p(\mu)\langle P_1P_2|O_i|B\rangle_F \tag{31}$$

Here $\langle P_1P_2|O_i|B\rangle_F$ is the factorized matrix element and can be factorizes into a form factor times a decay constant. The explicit expressions for the decay amplitudes of $B \to P_1P_2$ can be found in Ref. [23]. For the processes involving $\eta^{(\prime)}$ in the final states, Ali *et al.* [23] included the terms directly proportional to the so-called charm decay constant $f^c_{\eta^{(\prime)}}$ of the $\eta^{(\prime)}$ meson in the decay amplitudes. We ignored these terms here because they are very small in size. For the charmless B meson decays considered here, the hadronic matrix elements $\langle P_1P_2|O^c_{1,2}|B\rangle_F$ have no contributions. Following Beneke *et al.* [26], every coefficient $a_i(P_1, P_2)$ ($i = 1$ to 10) can be split into two parts:

$$a_i(P_1, P_2) = a_{i,I}(P_1, P_2) + a_{i,II}(P_1, P_2) \tag{32}$$

with

[2] For more details of various contributions and the corresponding Feynman loops, see, for example, Refs. [26,27] and references therein.

$$
\begin{aligned}
a_{1,I} &= C_1 + \frac{C_2}{N_c}\left[1 + \frac{C_F\alpha_s}{4\pi}V_{P_2}\right], \qquad a_{1,II} = \frac{C_2}{N_c}\frac{C_F\pi\alpha_s}{N_c}H_{P_1P_2}, \qquad a_{2,I} = C_2 + \frac{C_1}{N_c}\left[1 + \frac{C_F\alpha_s}{4\pi}V_{P_1}\right],\\
a_{2,II} &= \frac{C_1}{N_c}\frac{C_F\pi\alpha_s}{N_c}H_{P_2P_1}, \qquad a_{3,I} = C_3 + \frac{C_4}{N_c}\left[1 + \frac{C_F\alpha_s}{4\pi}V_{P_1}\right], \qquad a_{3,II} = \frac{C_4}{N_c}\frac{C_F\pi\alpha_s}{N_c}H_{P_2P_1},\\
a^p_{4,I} &= C_4 + \frac{C_3}{N_c}\left[1 + \frac{C_F\alpha_s}{4\pi}V_{p_2}\right] + \frac{C_F\alpha_s}{4\pi}\frac{P^p_{p_2,2}}{N_c}, \qquad a_{4,II} = \frac{C_3}{N_c}\frac{C_F\pi\alpha_s}{N_c}H_{P_1P_2},\\
a_{5,I} &= C_5 + \frac{C_6}{N_c}\left[1 + \frac{C_F\alpha_s}{4\pi}(-V'_{P_1})\right], \qquad a_{5,II} = \frac{C_6}{N_c}\frac{C_F\pi\alpha_s}{N_c}(-H'_{P_2P_1}), \qquad (33)\\
a^p_{6,I} &= C_6 + \frac{C_5}{N_c}\left[1 - 6.\frac{C_F\alpha_s}{4\pi}\right] + \frac{C_F\alpha_s}{4\pi}\frac{P^p_{p_2,3}}{N_c}, \qquad a_{6,II} = 0, \qquad a_{7,I} = C_7 + \frac{C_8}{N_c}\left[1 + \frac{C_F\alpha_s}{4\pi}(-V'_{P_1})\right],\\
a_{7,II} &= \frac{C_8}{N_c}\frac{C_F\pi\alpha_s}{N_c}(-H'_{P_2P_1}), \qquad a^p_{8,I} = C_8 + \frac{C_7}{N_c}\left[1 - 6\frac{C_F\alpha_s}{4\pi}\right] + \frac{\alpha_{em}}{9\pi}\frac{P^{p,\mathrm{EW}}_{p_2,3}}{N_c},\\
a_{8,II} &= 0, \qquad a_{9,I} = C_9 + \frac{C_{10}}{N_c}\left[1 + \frac{C_F\alpha_s}{4\pi}V_{P_1}\right], \qquad a_{9,II} = \frac{C_{10}}{N_c}\frac{C_F\pi\alpha_s}{N_c}H_{P_2P_1},\\
a^p_{10,I} &= C_{10} + \frac{C_9}{N_c}\left[1 + \frac{C_F\alpha_s}{4\pi}V_{P_2}\right] + \frac{\alpha_{em}}{9\pi}\frac{P^{p,\mathrm{EW}}_{p_2,2}}{N_c}, \qquad a_{10,II} = \frac{C_9}{N_c}\frac{C_F\pi\alpha_s}{N_c}H_{P_1P_2},
\end{aligned}
$$

where $N_c = 3$, $C_F = 4/3$, $a_{i,I} \equiv a_{i,I}(\mu)$, and $a_{i,II} \equiv a_{i,II}(\mu_h)$ with $\mu \sim m_b$ and $\mu_h = \sqrt{\Lambda_h \mu}$ with $\Lambda_h = 0.5$ GeV as in Ref. [26]. The terms $V_P^{(\prime)}$ result from the vertex corrections, $H^{(\prime)}_{P_1,P_2}$ describes the hard-scattering spectator contributions, $P^p_{P_2,2}$ and $P^p_{P_2,3}$ ($P^{p,\mathrm{EW}}_{P_2,2}$ and $P^{p,\mathrm{EW}}_{P_2,3}$) arise from the QCD (electroweak) penguin contributions and the contributions from dipole operator O_{8g} ($O_{7\gamma}$). For the four penguin terms, the subscript two or three indicates the twist of the corresponding projection. The explicit expressions of the functions $V_P^{(\prime)}$, $H^{(\prime)}_{P_1,P_2}$, $P^p_{P_2,2}$, $P^p_{P_2,3}$, $P^{p,\mathrm{EW}}_{P_2,2}$, and $P^{p,\mathrm{EW}}_{P_2,3}$ can be found in Ref. [26].

In QCD FA, the nonfactorizable power-suppressed contributions are neglected. However, the hard-scattering spectator interactions and annihilation diagrams cannot be neglected because of the chiral enhancement. Since they give rise to infrared endpoint singularities when computed perturbatively, they can only be estimated in a model-dependent way and with a large uncertainty. In Refs. [26,27] these contributions are parameterized by two complex quantities, X_H and X_A,

$$X_{H,A} = (1 + \rho_{H,A}e^{i\phi_{H,A}})\ln\frac{m_B}{\Lambda_h} \qquad (34)$$

where $\Lambda_h = 0.5$ GeV, $\phi_{H,A}$ are free phases in the range $[-180°, 180°]$, and $\rho_{H,A}$ are real parameters varying within $[0, 1]$. In this paper, we use the formulas as given in Ref. [26] directly to estimate the annihilation contributions to specific final state. Under the convention of Ref. [26], the annihilation amplitude can be written as

$$\mathcal{A}^{\mathrm{ann}}(B \to P_1P_2) \propto \frac{G_F}{\sqrt{2}}\sum_{p=u,c}\sum_i V_{pb}V^*_{pq}f_Bf_{P_1}f_{P_2}b_i(P_1,P_2) \qquad (35)$$

where f_B, f_M are the decay constants of B meson and final-state hadrons, respectively. The coefficients $b_i(P_1, P_2)$ describe the annihilation contributions and generally depend on quantity X_A. For explicit expressions of coefficients b_i one can see Ref. [26].

Now the total decay amplitudes can be written as

$$\mathcal{A}(B \to P_1P_2) = \mathcal{A}^f(B \to P_1P_2) + \mathcal{A}^{\mathrm{ann}}(B \to P_1P_2), \qquad (36)$$

the corresponding branching ratio then takes the form

$$\mathcal{B}(B \to P_1P_2) = \tau_B\frac{|P_c|}{8\pi M_B^2}|\mathcal{A}(B \to P_1P_2)|^2, \qquad (37)$$

where τ_B is the B meson lifetimes, and $|P_c|$ is the absolute values of two final-state hadrons' momentum in the B rest frame. For the CP-conjugated decay modes, the branching ratios can be obtained by replacement of $\lambda_p \to \lambda_p^*$ in the expressions of decay amplitudes.

The new physics contributions to the branching ratios of $B \to PP$ decays will be included by using the Wilson coefficients C_i with the inclusion of the new physics parts as described in Eqs. (14), (15), and (24)–(27).

IV. NUMERICAL CALCULATIONS

In this section, we first give the input parameters needed in numerical calculations, and then present the numerical results and make some theoretical analysis.

A. Input parameters

(i) The parameters $(A, \lambda, \bar{\rho}, \bar{\eta})$ in Wolfenstein parametrization of the CKM matrix. At present, the parameters A and λ have been well determined by experiments. In numerical calculation, we will use $A = 0.854$, $\lambda = 0.2196$, $\overline{\rho} = 0.22 \pm 0.10$, and $\overline{\eta} = 0.35 \pm 0.05$ as given in Ref. [31].

(ii) Quark masses. When calculating the decay amplitudes, the pole and current quark masses will be used. For the former, we will use

$$m_u = 4.2 \text{ Mev}, \qquad m_c = 1.5 \text{ Gev}, \qquad m_t = 175 \text{ Gev},$$

$$m_d = 7.6 \text{ Mev}, \qquad m_s = 0.122 \text{ Gev}, \qquad m_b = 4.62 \text{ Gev}.$$

The current quark mass depends on the renormalization scale. In the $\overline{MS}$ scheme and at a scale of 2 GeV, we fix

$$\overline{m}_u(2 \text{ Gev}) = 2.4 \text{ Mev}, \qquad \overline{m}_d(2 \text{ Gev}) = 6 \text{ Mev},$$

$$\overline{m}_s(2 \text{ Gev}) = 105 \text{ Mev}, \qquad \overline{m}_b(\overline{m}_b) = 4.26 \text{ Gev},$$

as given in Particle Data Group 2002 [31], and then employ the formulae in Ref. [37]

$$\overline{m}(\mu) = \overline{m}(\mu_0)\left[\frac{\alpha_s(\mu)}{\alpha_s(\mu_0)}\right]^{\gamma_m^{(0)}/2\beta_0}\left[1 + \left(\frac{\gamma_m^{(1)}}{2\beta_0} - \frac{\beta_1\gamma_m^{(0)}}{2\beta_0^2}\right)\frac{\alpha_s(\mu) - \alpha_s(\mu_0)}{4\pi}\right] \tag{38}$$

to obtain the current quark masses at any scale. The definitions of α_s, $\gamma_m^{(0)}$, $\gamma_m^{(1)}$, β_0, and β_1 can be found in Ref. [37].

(iii) Form factors and decay constants. Following Ref. [27], we also use

$$F_0^{B\to\pi}(0) = 0.28 \pm 0.05, \qquad F_0^{B\to k}(0) = 0.34 \pm 0.05. \tag{39}$$

The decay constants of π, k and B are [26]

$$f_\pi = 131 \text{ Mev}, \qquad f_k = 160 \text{ Mev}, \qquad f_B = 180 \text{ Mev}$$

For η and η', mixing happens between them. The decay constants of them can be parameterized by f_q, f_s and the mixing angle ϕ of $\eta - \eta'$ [42]

$$f_\eta^u = f_\eta^d = f_\eta^q \cos\phi, f_\eta^s = -f_s \sin\phi$$

$$f_{\eta'}^u = f_{\eta'}^d = f_\eta^q \sin\phi, f_{\eta'}^s = f_s \cos\phi$$

with

$$f_q = (1.07 \pm 0.02)f_\pi, \qquad f_s = (1.34 \pm 0.06)f_\pi, \qquad \phi = (39.3 \pm 1.0)^\circ$$

Similarly, the form factors $F_0^{B\to\eta}(0)$ and $F_0^{B\to\eta'}(0)$ are parameterized as in Ref. [42].

(iv) For the parameters $\rho_{H,A}$ and $\phi_{H,A}$, we do not consider the variation of these parameters but fix

$$\rho_A = 0.05, \qquad \phi_A = 10^\circ, \qquad \rho_H = 0, \qquad \phi_H = 0^\circ$$

in numerical calculation. For the parameter λ_B appeared in the B meson light cone distribution amplitude, we also take $\lambda_B = (350 \pm 150)$ Mev as in Ref. [26].

(v) For the well-known $\pi, K, \eta^{(\prime)}$ and B meson masses, as well as the B meson lifetimes, we use the values as given in Ref. [31].

(vi) The SUSY parameters at electroweak scale. Within the parameter space still allowed by known constraints from the data [16,18,43] [such as the strong constraints from the precise measurements of $Br(B \to X_s\gamma)$], we choose two sets of SUSY parameters of the mSGURA model at the high unification energy scale as listed in Table II. The resulting masses of charged-Higgs boson and charginos obtained by using the program SUSPECT V 2.1 [32] are also given in Table II.

TABLE II. Two sets of SUSY parameters to be used in numerical calculation. And the corresponding mass spectrum of charged-Higgs boson and the charginos. All masses are in unit of GeV.

Cases	$\tan\beta$	$m_{1/2}$	m_0	A_0	sgn(μ)	$m_{H^\pm}$	$m_{\chi_1^\pm}$	$m_{\chi_2^\pm}$
Case-A	2	300	300	0	$-$	782.3	247.0	595.9
Case-B	40	150	369	-400	$+$	330.2	109.6	312.3

In numerical calculations, we always use the central values of above input parameters unless explicitly stated otherwise.

B. Wilson coefficients: Case A and B

From explicit calculations, we find that the SUSY corrections to $B \to PP$ decays are mostly induced by the new physics parts of the $C_{7\gamma}$ and C_{8g}, while the coefficients $C_k^{\rm NP}$ $(k = 3, 4, 5, 6)$ are indeed too small to modify their SM counterparts effectively. The numerical results show that the $C_{7\gamma}(m_b)$ and $C_{8g}(m_b)$ in the mSUGRA model can be quite different from that in the SM, and can even have the opposite sign compared with their SM counterparts.

1. Case A

We first consider the Case A. For the SUSY part, since we take the mixing matrix Γ^U and Γ^D as given in Eq. (28), the Feynman diagrams induced by the gluino and neutralino exchanges do not contribute to the quark level decays $b \to (s, d)\gamma$ and $b \to (s, d)g$. To a precision of

$\mathcal{O}(10^{-5})$, the SUSY contributions to $C_k (k = 3, 4, 5, 6)$ at the scale m_W are the same for both $b \to s$ and $b \to d$ transitions. The contributions from the gauge boson $W^{\pm}$, the charged-Higgs and the charginos are

$$C_k^{\rm SM}(m_W) = \{0.00155, -0.00197, 0.00066, -0.00197\}, \tag{40}$$

$$C_k^{H^{\pm}}(m_W) = \{-0.00001, 0.00004, -0.00001, 0.00004\}, \tag{41}$$

$$C_k^{\tilde{\chi}^{\pm}}(m_w) = \{0, 0.00003, 0, 0.00003\}. \tag{42}$$

For $C_{7\gamma}(M_W)$ and $C_{8g}(M_W)$, the NLO level numerical results are

$$C_{7\gamma}(m_W) = \begin{cases} \underbrace{-0.2175}_{C_{7\gamma}^{\rm SM}(m_W)} \underbrace{-0.0422}_{C_{7\gamma}^{H^{\pm}}(m_W)} \underbrace{-0.0007 - 0.0002I}_{C_{7\gamma}^{\tilde{\chi}^{\pm}}(m_W)} = -0.2604 - 0.0002I, & b \to d \\ \underbrace{-0.2175}_{C_{7\gamma}^{\rm SM}(m_W)} \underbrace{-0.0422}_{C_{7\gamma}^{H^{\pm}}(m_W)} \underbrace{-0.0009 - 0.0002I}_{C_{7\gamma}^{\tilde{\chi}^{\pm}}(m_W)} = -0.2606 - 0.0002I, & b \to s \end{cases} \tag{43}$$

$$C_{8g}(m_W) = \begin{cases} \underbrace{-0.1178}_{C_{8g}^{\rm SM}(m_W)} \underbrace{-0.0473}_{C_{8g}^{H^{\pm}}(m_w)} \underbrace{-0.0002}_{C_{8g}^{\tilde{\chi}^{\pm}}(m_W)} = -0.1653, & b \to d \\ \underbrace{-0.1178}_{C_{8g}^{\rm SM}(m_W)} \underbrace{-0.0473}_{C_{8g}^{H^{\pm}}(m_w)} \underbrace{-0.0002 - 0.0001I}_{C_{8g}^{\tilde{\chi}^{\pm}}(m_W)} = -0.1653 - 0.0001I, & b \to s \end{cases} \tag{44}$$

The new physics contributions to $C_k(M_W)$ ($k = 3, 4, 5, 6$) are clearly two orders smaller than their SM counterparts and therefore can be neglected safely. For $C_{7\gamma}(M_W)$ and $C_{8g}(M_W)$ the charged-Higgs contribution is dominant over the chargino contribution, but still much smaller than their SM counterparts. Obviously the Case A is not phenomenologically interesting, since the SUSY effect is too small to be separated from the SM contribution though experimental measurements.

2. Case B

Now we turn to Case B. For this case, the SUSY contributions to $C_k (k = 3, 4, 5, 6)$ are still negligibly small: (a) the charged-Higgs contributions are at the $\mathcal{O}(10^{-7})$ level; and (b) the chargino contributions are at the $\mathcal{O}(10^{-5})$ for both $b \to s$ and $b \to d$ transitions.

For $C_{7\gamma}(M_W)$ and $C_{8g}(M_W)$, however, the SUSY contributions are significant:

$$C_{7\gamma}(m_W) = \begin{cases} \underbrace{-0.2175}_{C_{7\gamma}^{\rm SM}(m_W)} \underbrace{-0.1128}_{C_{7\gamma}^{H^{\pm}}(m_W)} \underbrace{+1.0111 + 0.0063I}_{C_{7\gamma}^{\tilde{\chi}^{\pm}}(m_W)} = 0.6808 + 0.0063I, & b \to d \\ \underbrace{-0.2175}_{C_{7\gamma}^{\rm SM}(m_W)} \underbrace{-0.1128}_{C_{7\gamma}^{H^{\pm}}(m_W)} \underbrace{+1.0193 + 0.0091I}_{C_{7\gamma}^{\tilde{\chi}^{\pm}}(m_W)} = 0.6890 + 0.0009I, & b \to s \end{cases} \tag{45}$$

$$C_{8g}(m_W) = \begin{cases} \underbrace{-0.1178}_{C_{8g}^{\rm SM}(m_W)} \underbrace{-0.1103}_{C_{8g}^{H^{\pm}}(m_w)} \underbrace{+0.4622 + 0.0007I}_{C_{8g}^{\tilde{\chi}^{\pm}}(m_W)} = 0.2341 + 0.0007I, & b \to d \\ \underbrace{-0.1178}_{C_{8g}^{\rm SM}(m_W)} \underbrace{-0.1103}_{C_{8g}^{H^{\pm}}(m_w)} \underbrace{+0.4631 + 0.0010I}_{C_{8g}^{\tilde{\chi}^{\pm}}(m_W)} = 0.2350 + 0.0010I, & b \to s \end{cases} \tag{46}$$

At the lower scale m_b, they are

$$C_{7\gamma}(m_b) = \begin{cases} \underbrace{-0.3067}_{C_{7\gamma}^{\rm SM}(m_b)} \underbrace{+0.5896 + 0.0039I}_{C_{7\gamma}^{H^{\pm}}(m_b) + C_{7\gamma}^{\tilde{\chi}^{\pm}}(m_b)} = 0.2829 + 0.0039I, & b \to d \\ \underbrace{-0.3067}_{C_{7\gamma}^{\rm SM}(m_b)} \underbrace{+0.5947 + 0.0058I}_{C_{7\gamma}^{H^{\pm}}(m_b) + C_{7\gamma}^{\tilde{\chi}^{\pm}}(m_b)} = 0.2880 + 0.0058I, & b \to s \end{cases} \tag{47}$$

$$C_{8g}(m_b) = \begin{cases} \underbrace{-0.1500}_{C_{8g}^{\rm SM}(m_b)} \underbrace{+0.2449 + 0.0005I}_{C_{8g}^{H^{\pm}}(m_b) + C_{8g}^{\tilde{\chi}^{\pm}}(m_b)} = 0.0949 + 0.0005I, & b \to d \\ \underbrace{-0.1500}_{C_{8g}^{\rm SM}(m_b)} \underbrace{+0.2455 + 0.0007I}_{C_{8g}^{H^{\pm}}(m_b) + C_{8g}^{\tilde{\chi}^{\pm}}(m_b)} = 0.0955 + 0.0007I, & b \to s \end{cases} \tag{48}$$

From the numerical values in Eqs. (45)–(48), one can see that

(i) At the scale M_W, the charged-Higgs contributions to both $C_{7\gamma}$ and C_{8g} have the same sign with their SM counterparts, and are comparable in size with them. The chargino contributions, however, have an opposite sign with $C_{7\gamma}^{\rm SM}$ and $C_{8g}^{\rm SM}$, and much larger in size than them.

(ii) At both energy scales m_W and m_b, the net new physics contributions to $C_{7\gamma}$ and C_{8g} are always positive and consequently cancel their SM counterpart. The total value of these two coefficients therefore become positive after the combination of the SM and the new physics parts.

(iii) It is easy to understand why the new physics contributions in case-B are much larger than those in Case A. In Case A, the new physics contributions from both charged-Higgs boson and charginos are negligibly small. In Case B, however, we have many light charged-Higgs boson and charginos, which leads to large SUSY contributions. After the cancellation among the SM and SUSY contributions, the net value of $C_{7\gamma}$ and C_{8g} is positive.

(iv) In Case B, though $C_{7\gamma}(m_b)$ received a large supersymmetric correction and has the opposite sign with its SM counterpart, its absolute value changes a little and makes the theoretical prediction for the branching ratio of $b \to s\gamma$ decay still consistent with the data. The reason is rather simple: the branching ratio $Br(b \to s\gamma)$ is basically proportional to $|C_{7\gamma}(m_b)|^2$.

C. Branching ratios: data and theoretical prediction

Using the decay amplitudes as given in Refs. [23,28] and the coefficients a_i in Eq. (33), it is straightforward to calculate the branching ratios of those 21 $B \to PP$ decay modes in the SM and mSUGRA model.

In order to show more details about the ways to include the SUSY contributions, we present here, as an example, the calculations for the branching ratio $Br(B \to \pi^+ K^-)$. The decay amplitudes of $B^0 \to \pi^+ K^-$ are

$$\mathcal{A}^f(B^0 \to \pi^+ K^-) = -i\frac{G_F}{\sqrt{2}} f_k F_0^{B\to\pi}(m_B^2 - m_\pi^2)\{V_{ub}V_{us}^*[a_1 + a_4^u + a_{10}^u + (a_6^u + a_8^u)R_4] + V_{cb}V_{cs}^*[a_4^c + a_{10}^c + (a_6^c + a_8^c)R_4]\}, \tag{49}$$

$$\mathcal{A}^{\rm ann}(B^0 \to \pi^+ K^-) = -i\frac{G_F}{\sqrt{2}} f_B f_\pi f_k\left\{-V_{tb}V_{ts}^*\left[b_3(K\pi) - \frac{1}{2}b_3^{\rm EW}(K,\pi)\right]\right\} \tag{50}$$

with

$$R_4 = \frac{2m_K^2}{(m_b - m_u)(m_u + m_d)}, \tag{51}$$

where the coefficients a_i^p have been given in Eq. (33), the coefficients $b_i(P_1, P_2)$ describe the annihilation contributions [26]. Because of the strong Cabbibo suppression ($|V_{ub}V_{us}^*|^2 \propto \lambda^4$) on the "tree" contribution (the a_1 term), the four $B \to \pi K$ decays are QCD penguin-dominant decay modes, and strongly depend on "large" coefficients a_4^p and a_6^p.

We follow the same mechanism as described in Refs. [23,26] to include the SUSY contributions to $B \to PP$ decays.

As mentioned previously, the SUSY contributions to the Wilson coefficients of the 4-quark penguin operators are very small and have been neglected. The large new magnetic penguin contributions in the mSUGRA model can manifest themselves as radiative corrections to the Wilson coefficients $C_{4,6,8,10}$ (or equivalently to $a_{j,I}^p$ with $j = 4, 6, 8, 10$ and $p = u, c$) and contained in the quantities $P_{P_2,2}^p$, $P_{P_2,2}^{p,\rm EW}$, $P_{P_2,3}^p$, and $P_{P_2,3}^{p,\rm EW}$.

For $B \to \pi^+ K^-$ decay, for example, the quantities $P_{K,2}^p$ and $P_{K,2}^{p,\rm EW}$ can be written as [26]

$$P_{K,2}^p = C_1\left[\frac{4}{3}\ln\frac{m_b}{\mu} + \frac{2}{3} - G_k(s_p)\right] + C_3\left[\frac{8}{3}\ln\frac{m_b}{\mu} + \frac{4}{3} - G_K(0) - G_K(1)\right] + (C_4 + C_6)\left[\frac{20}{3}\ln\frac{m_b}{\mu} - 3G_K(0) - G_K(s_c) - G_K(1)\right] - 6C_{8g}^{\rm eff}(1 + \alpha_1^K + \alpha_2^K), \tag{52}$$

$$P_{K,2}^{p,\rm EW} = (C_1 + N_c C_2)\left[\frac{4}{3}\ln\frac{m_b}{\mu} + \frac{2}{3} - G_K(s_p)\right] - 9C_{7\gamma}^{\rm eff}(1 + \alpha_1^K + \alpha_2^K), \tag{53}$$

where $s_u = 0$, $s_c = m_c^2/m_b^2$ are mass ratios involved in the evaluation of penguin diagrams, $\alpha_1^K = 0.3 \pm 0.3$ and $\alpha_2^K = 0.1 \pm 0.3$ are Gegenbauer moments for K meson [26]. $C_{7\gamma}^{\rm eff} = C_{7\gamma} - \frac{1}{3}C_5 - C_6$ and $C_{8g}^{\rm eff} = C_{8g} + C_5$ are the so-called "effective " Wilson coefficients. The explicit expressions of the functions $G_K(0)$, $G_K(1)$, and $G_K(s_p)$ can be found easily in Ref. [26]. The twist-3 quantities $P_{P_2,3}^p$ and $P_{P_2,3}^{p,\rm EW}$ receive the SUSY corrections in the same way as $P_{P_2,2}^p$ and $P_{P_2,2}^{p,\rm EW}$.

From Eqs. (33), (52), and (53), and the numerical results as listed in Table III, one can see that

(i) After the inclusion of SUSY contributions, the effective coefficients $C_{7\gamma}^{\rm eff}$ and $C_{8g}^{\rm eff}$ changed their sign from negative to positive. The real parts of the coefficients $a_{4,I}^p$ and $a_{6,I}^p$ are consequently

TABLE III. The coefficients $C_{7\gamma}^{\rm eff}(\mu)$, $C_{8g}^{\rm eff}(\mu)$, and $a_{j,I}^p$ ($j = 4, 6, 8, 10$ and $p = u, c$) for $B \to \pi K$ decays in the SM and the Case B of the mSUGRA model.

	$\mu = m_b/2$		$\mu = m_b$		$\mu = 2m_b$	
	SM	mSUGRA	SM	mSUGRA	SM	mSUGRA
$C_{7\gamma}^{\rm eff}(\mu)$	-0.276	$+0.221$	-0.270	$+0.325$	-0.258	$+0.422$
$C_{8g}^{\rm eff}(\mu)$	-0.155	$+0.058$	-0.142	$+0.104$	-0.130	$+0.145$
$a_{4,I}^u \times 10^3$	$-24.3 - 17.4i$	$-41.7 - 17.4i$	$-23.9 - 14.4i$	$-39.8 - 14.4i$	$-22.6 - 12.3i$	$-37.4 - 12.3i$
$a_{4,I}^c \times 10^3$	$-31.4 - 12.1i$	$-48.8 - 12.1i$	$-29.0 - 10.4i$	$-45.0 - 10.4i$	$-26.9 - 9.0i$	$-41.7 - 9.0i$
$a_{6,I}^u \times 10^3$	$-54.0 - 15.8i$	$-58.3 - 15.8i$	$-40.2 - 13.6i$	$-43.9 - 13.6i$	$-32.3 - 11.9i$	$-35.7 - 11.9i$
$a_{6,I}^c \times 10^3$	$-60.4 - 2.9i$	$-64.5 - 2.9i$	$-44.8 - 3.8i$	$-49.0 - 3.8i$	$-36.0 - 4.0i$	$-39.5 - 4.0i$
$a_{8,I}^u \times 10^4$	$4.7 - 0.6i$	$3.3 - 0.6i$	$3.0 - 1.1i$	$1.4 - 1.1i$	$1.8 - 1.4i$	$-0.1 - 1.4i$
$a_{8,I}^c \times 10^4$	$4.6 - 0.3i$	$3.2 - 0.3i$	$2.7 - 0.5i$	$1.1 - 0.5i$	$1.4 - 0.6i$	$-0.5 - 0.6i$
$a_{10,I}^u \times 10^4$	$-12.0 + 12.4i$	$-18.0 + 12.4i$	$-13.0 + 8.6i$	$-19.9 + 8.6i$	$-14.9 + 6.3i$	$-23.0 + 6.3i$
$a_{10,I}^c \times 10^4$	$-12.3 + 12.5i$	$-18.1 + 12.5i$	$-13.4 + 8.9i$	$-20.3 + 8.9i$	$-15.4 + 6.6i$	$-23.0 + 6.6i$

changed by about 60% and 10%, respectively, but the imaginary parts of $a_{j,I}^p$ remain unchanged.

(ii) Since the magnitude of coefficients $a_{4,I}^p$ and $a_{6,I}^p$ is larger than that of $a_{8,I}^p$ and $a_{10,I}^p$ by one or two orders, the new physics contributions to C_{8g} dominate the total new physics corrections.

(iii) Since only the coefficients $a_{j,I}^p$ for $j = 4, 6, 8, 10$ receive the SUSY contributions, one naturally expects a moderate or large new physics correction to those penguin-dominated B meson decays, such as $B \to K\pi$ and $B \to K\eta'$ processes. The tree-dominated decay modes, for example $B \to \pi\pi$ decays, remain basically unaffected.

For the phenomenologically interesting $B \to K\eta'$ decays and other penguin-dominated decay modes studied here, the large SUSY contributions will be included in the same way as for $B \to \pi^+ K^-$ decays.

Among 21 $B \to PP$ decay modes considered here, twelve of them have been measured so far. The individual measurements and the world average for the branching ratios of these decays [9] are shown in Table IV.

In Table V, we show the theoretical predictions for the CP-averaged branching ratios for $B \to PP$ decays in both the SM and the mSUGRA model (Case B), assuming $\mu = m_b/2, m_b$ and $2m_b$, respectively. And Br^{f+a} and Br^f denote the branching ratios with or without the inclusion

TABLE IV. Experimental data of the branching ratios for $B \to PP$ in unit of 10^{-6}, taken from the HFAG website [9]. For $\overline{B}^0 \to \overline{K}^0\eta$ decay, the *BABAR*'s result [44] will be used in our analysis.

Decay Modes	*BABAR*	Belle	CLEO	Average
$B^- \to \pi^- \overline{K}^0$	$22.3 \pm 1.7 \pm 1.1$	$22.0 \pm 1.9 \pm 1.1$	$18.8^{+3.7+2.1}_{-3.3-1.8}$	21.8 ± 1.4
$B^- \to \pi^0 K^-$	$12.8^{+1.2}_{-1.1} \pm 1.0$	$12.0 \pm 1.3^{+1.3}_{-0.9}$	$12.9^{+2.4+1.2}_{-2.2-1.1}$	$12.5^{+1.1}_{-1.0}$
$\overline{B}^0 \to \pi^+ K^-$	$17.9 \pm 0.9 \pm 0.7$	$18.5 \pm 1.0 \pm 0.7$	$18.0^{+2.3+1.2}_{-2.1-0.9}$	18.2 ± 0.8
$B^0 \to \pi^0 \overline{K}^0$	$11.4 \pm 1.7 \pm 0.8$	$11.7 \pm 2.3^{+1.2}_{-1.3}$	$12.8^{+4.0+1.7}_{-3.3-1.4}$	11.7 ± 1.4
$\overline{B}^0 \to \pi^+\pi^-$	$4.7 \pm 0.6 \pm 0.2$	$4.4 \pm 0.6 \pm 0.3$	$4.5^{+1.4+0.5}_{-1.2-0.4}$	4.6 ± 0.4
$B^- \to \pi^-\pi^0$	$5.5^{+1.0}_{-0.9} \pm 0.6$	$5.0 \pm 1.2 \pm 0.5$	$4.6^{+1.8+0.6}_{-1.6-0.7}$	5.2 ± 0.8
$\overline{B}^0 \to \pi^0\pi^0$	$2.1 \pm 0.6 \pm 0.3$	$1.7 \pm 0.6 \pm 0.2$	<4.4	1.9 ± 0.5
$B^- \to K^-\eta$	$3.4 \pm 0.8 \pm 0.2$	$5.3^{+1.8}_{-1.5} \pm 0.6$	$2.2^{+2.8}_{-2.2}$	3.7 ± 0.7
$B^- \to K^-\eta'$	$76.9 \pm 3.5 \pm 4.4$	$76 \pm 6 \pm 9$	$80^{+10}_{-9} \pm 7$	$77.6^{+4.6}_{-4.5}$
$\overline{B}^0 \to \overline{K}^0\eta$	$2.9 \pm 1.0 \pm 0.2$	<12	<9.3	$2.9 \pm 1.0 \pm 0.2$
$\overline{B}^0 \to \overline{K}^0\eta'$	$60.6 \pm 5.6 \pm 4.6$	$68 \pm 10^{+9}_{-8}$	$89 \pm ^{+18}_{-16} \pm 9$	$65.2^{+6.0}_{-5.9}$
$B^- \to \pi^-\eta$	$5.3 \pm 1.0 \pm 0.3$	$5.4^{+2.0}_{-1.7} \pm 0.6$	$1.2^{+2.8}_{-1.2}$	$4.9^{+0.9}_{-0.8}$
$B^- \to \pi^-\eta'$	<4.5	<7	<12	<4.5
$\overline{B}^0 \to \pi^0\eta$	<2.5		<2.9	<2.5
$\overline{B}^0 \to \pi^0\eta'$	<3.7		<5.7	<3.7
$\overline{B}^0 \to \eta\eta$	<2.8		<18	<2.8
$\overline{B}^0 \to \eta\eta'$	<4.6		<27	<4.6
$\overline{B}^0 \to \eta'\eta'$	<10		<47	<10
$B^- \to K^- K^0$	<2.5	<3.3	<3.3	<2.4
$\overline{B}^0 \to \overline{K}^0 K^0$	<1.8	<1.5	<3.3	<1.5
$\overline{B}^0 \to K^+ K^-$	<0.6	<0.7	<0.8	<0.6

TABLE V. The CP-averaged branching ratios of $B \to PP$ decays in the SM and THE minimal SUGRA model (in units of 10^{-6}) by using the central values of input parameters. Br^{f+a} and Br^f denote the results with or without the annihilation contributions.

Decays	$\mu = m_b/2$				$\mu = m_b$				$\mu = 2m_b$			
	SM		mSUGRA		SM		mSUGRA		SM		mSUGRA	
	Br^f	Br^{f+a}	Br^f	Br^{f+a}	Br^f	Br^{f+a}	Br^f	Br^{f+a}	Br^f	Br^{f+a}	Br^f	Br^{f+a}
$B^- \to \pi^- \overline{K}^0$	13.6	16.2	20.5	23.6	12.7	14.7	19.1	21.6	12.0	13.6	18.1	20.1
$B^- \to \pi^0 K^-$	8.1	9.3	11.8	13.4	7.6	8.6	11.2	12.4	7.3	8.1	10.7	11.7
$\overline{B}^0 \to \pi^+ K^-$	10.5	12.4	16.3	18.8	10.0	11.6	15.6	17.5	9.7	10.9	15.1	16.7
$B^0 \to \pi^0 \overline{K}^0$	4.4	5.3	7.1	8.3	4.1	4.8	6.6	7.6	3.9	4.5	6.3	7.0
$\overline{B}^0 \to \pi^+ \pi^-$	9.0	9.6	9.2	9.9	8.8	9.3	9.0	9.5	8.6	9.0	8.8	9.3
$B^- \to \pi^- \pi^0$	6.1	$\cdots$	6.1	$\cdots$	6.3	$\cdots$	6.3	$\cdots$	6.4	$\cdots$	6.4	$\cdots$
$\overline{B}^0 \to \pi^0 \pi^0$	0.35	0.39	0.43	0.47	0.31	0.32	0.37	0.39	0.31	0.31	0.36	0.37
$B^- \to K^- \eta$	2.7	2.7	3.6	3.6	2.7	2.7	3.6	3.6	2.5	2.6	3.4	3.5
$B^- \to K^- \eta'$	36.6	47.6	48.1	60.6	30.0	38.1	40.2	49.4	26.7	32.8	36.2	43.3
$\overline{B}^0 \to \overline{K}^0 \eta$	2.1	2.1	2.9	2.9	2.0	2.0	2.8	2.8	1.9	1.9	2.7	2.7
$\overline{B}^0 \to \overline{K}^0 \eta'$	34.6	44.5	45.1	56.3	28.3	35.4	37.5	45.7	24.9	30.3	33.8	39.8
$B^- \to \pi^- \eta$	4.53	4.46	4.82	4.76	4.42	4.38	4.70	4.68	4.44	4.42	4.73	4.72
$B^- \to \pi^- \eta'$	3.98	3.97	4.17	4.17	3.73	3.73	3.91	3.92	3.69	3.69	3.86	3.86
$\overline{B}^0 \to \pi^0 \eta$	0.33	0.32	0.43	0.42	0.29	0.29	0.39	0.39	0.28	0.28	0.37	0.37
$\overline{B}^0 \to \pi^0 \eta'$	0.32	0.32	0.38	0.39	0.25	0.25	0.31	0.31	0.22	0.22	0.27	0.27
$\overline{B}^0 \to \eta \eta$	0.20	0.29	0.23	0.33	0.19	0.27	0.23	0.31	0.21	0.27	0.24	0.31
$\overline{B}^0 \to \eta \eta'$	0.35	0.42	0.39	0.46	0.32	0.37	0.36	0.41	0.33	0.37	0.37	0.41
$\overline{B}^0 \to \eta' \eta'$	0.18	0.30	0.20	0.32	0.16	0.25	0.17	0.27	0.16	0.24	0.17	0.26
$B^- \to K^- K^0$	0.69	0.82	0.96	1.11	0.63	0.73	0.88	1.00	0.58	0.66	0.83	0.92
$\overline{B}^0 \to \overline{K}^0 K^0$	0.63	0.83	0.88	1.11	0.57	0.72	0.80	0.98	0.53	0.64	0.75	0.89
$\overline{B}^0 \to K^+ K^-$	$\cdots$	0.06	$\cdots$	0.06	$\cdots$	0.03	$\cdots$	0.03	$\cdots$	0.02	$\cdots$	0.02

of annihilation contributions, respectively. It is evident that some decay modes have strong $\mu -$ dependence, and the annihilation contributions can also be significant for $B \to K\pi$ and $B \to K\eta'$ decays. In the following subsections, we present the numerical results and show the dominant theoretical errors induced by the uncertainties of input parameters, and focus on those well-measured decay channels.

D. $B \to \pi\pi$ and $K\pi$ decays

The three $B \to \pi\pi$ decays are tree-dominated decay modes. The central values and the major errors of the branching ratios (in units of 10^{-6}) in the SM and the mSUGRA model are

$$Br(\overline{B}^0 \to \pi^+\pi^-) = \begin{cases} 9.3 \pm 0.3(\mu)^{+3.7}_{-3.1}(F_0)^{+0.9}_{-1.6}(\gamma) & \text{in SM,} \\ 9.5 \pm 0.3(\mu)^{+3.8}_{-3.2}(F_0)^{+1.0}_{-1.8}(\gamma) & \text{in mSUGRA,} \end{cases} \tag{54}$$

$$Br(B^- \to \pi^-\pi^0) = \begin{cases} 6.3^{+0.2}_{-0.1}(\mu)^{+2.2}_{-1.9}(F_0)^{+0.0}_{-0.2}(\gamma) & \text{in SM,} \\ 6.3^{+0.2}_{-0.1}(\mu)^{+2.2}_{-1.9}(F_0)^{+0.0}_{-0.2}(\gamma) & \text{in mSUGRA,} \end{cases} \tag{55}$$

$$Br(\overline{B}^0 \to \pi^0\pi^0) = \begin{cases} 0.32^{+0.07}_{-0.01}(\mu)^{+0.09}_{-0.08}(F_0)^{+0.14}_{-0.11}(\gamma) & \text{in SM,} \\ 0.39^{+0.08}_{-0.02}(\mu)^{+0.12}_{-0.10}(F_0)^{+0.18}_{-0.14}(\gamma) & \text{in mSUGRA,} \end{cases} \tag{56}$$

where the three major errors are induced by the uncertainties $m_b/2 \le \mu \le 2m_b$, $F_0^{B\to\pi} = 0.28 \pm 0.05$ and $\gamma = 60° \pm 20°$.

Figure 2 shows the γ dependence of the branching ratios for three $B \to \pi\pi$ decays. The dots and dashed curves correspond to the central values of the theoretical prediction in the SM and the mSUGRA model,[3] respectively. The horizontal slashed bands show the data as given in Table IV.

[3]The central values of all input parameters except for the CKM angle γ are used in this and other similar figures. The theoretical uncertainties are not shown in all such kinds of figures.

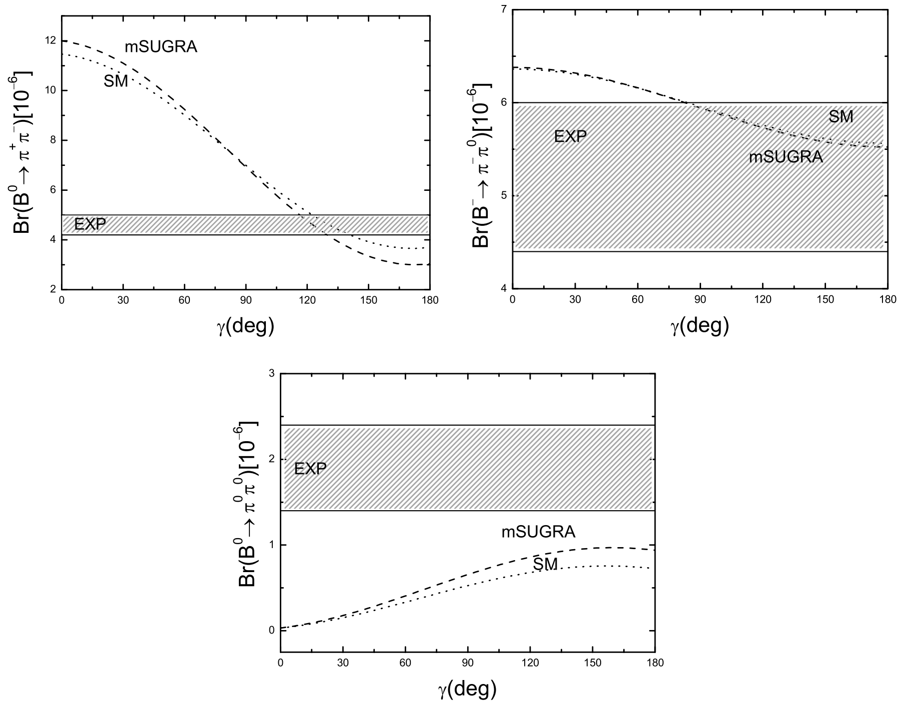

FIG. 2. The γ dependence of the branching ratios of $B \to \pi\pi$ decays in the SM and mSUGRA model. The dots and solid curves show the central values of the SM and mSUGRA predictions. The horizontal gray bands show the corresponding experimental measurements as given in Table III.

From Fig. 2 and the numerical results as given in Eqs. (54)–(56), one can see that

(i) For these tree-dominated decays, the SUSY corrections considered here are very small.

(ii) The theoretical predictions strongly depend on the value of the form factor $F_0^{B\to\pi}$.

(iii) For $B^0 \to \pi^0\pi^0$ decay, the theoretical prediction in QCD factorization is about 5 times smaller than the measured value and cannot become consistent with the data within the whole parameter space.

(iv) The central value of $Br(B^0 \to \pi^+\pi^-)$ is much larger than the data, but can become consistent with the data if one uses a smaller form factor $F_0^{B\to\pi}$ or a large angle $\gamma \sim 120°$. But a small $F_0^{B\to\pi}$ is disfavored by the large measured decay rates for $B \to \pi^0\pi^0$ and $K\pi$ decay modes, while a large γ around 120° is also in conflict with the global fit result $40^0 < \gamma < 78°$ at 95% confidence level [45] and the latest direct experimental measurement $\gamma = 81° \pm 19°(\text{stat.}) \pm 13°(\text{sys.}) \pm 11°(\text{model})$ [46].

In the SM, the four $B \to K\pi$ decays are dominated by the $b \to sg$ gluonic penguin diagrams, with additional contributions from $b \to u$ tree and electroweak penguin diagrams. For these decay modes, although the SM predictions can become consistent with the measured values after considering the still large theoretical uncertainties, the central values of the SM prediction are indeed much smaller than the measured values even after the inclusion of annihilation contributions. In the mSUGRA model, the new penguin diagrams induced by new particles can contribute effectively to $B \to K\pi$ decays. The numerical results (in unit of 10^{-6}) are

$$Br(B^- \to \pi^-\overline{K}^0) = \begin{cases} 14.7^{+1.4}_{-1.1}(\mu)^{+5.3}_{-4.8}(F_0)^{+0.1}_{-0.2}(\gamma)^{+4.5}_{-2.8}(\bar{m}_s) & \text{in SM,} \\ 21.6^{+2.0}_{-1.5}(\mu)^{+7.9}_{-6.6}(F_0)^{+0.2}_{-0.3}(\gamma)^{+5.8}_{-3.6}(\bar{m}_s) & \text{in mSUGRA,} \end{cases} \tag{57}$$

$$Br(B^- \to \pi^0 K^-) = \begin{cases} 8.6^{+0.7}_{-0.5}(\mu)^{+3.4}_{-2.6}(F_0)^{+1.5}_{-1.1}(\gamma)^{+2.3}_{-1.4}(\bar{m}_s) & \text{in SM,} \\ 12.4^{+1.0}_{-0.7}(\mu)^{+4.4}_{-3.8}(F_0)^{+1.7}_{-1.2}(\gamma)^{+3.0}_{-1.9}(\bar{m}_s) & \text{in mSUGRA,} \end{cases} \tag{58}$$

$$Br(\overline{B}^0 \to \pi^+ K^-) = \begin{cases} 11.6^{+0.9}_{-0.7}(\mu)^{+4.2}_{-3.5}(F_0)^{+1.9}_{-1.3}(\gamma)^{+3.0}_{-1.9}(\bar{m}_s) & \text{in SM,} \\ 17.5^{+1.3}_{-0.9}(\mu)^{+6.4}_{-5.4}(F_0)^{+2.3}_{-1.6}(\gamma)^{+4.8}_{-3.0}(\bar{m}_s) & \text{in mSUGRA} \end{cases} \tag{59}$$

$$Br(B^0 \to \pi^0 \overline{K}^0) = \begin{cases} 4.8^{+0.5}_{-0.4}(\mu)^{+1.8}_{-1.5}(F_0)^{+0.2}_{-0.3}(\gamma)^{+1.8}_{-1.1}(\bar{m}_s) & \text{in SM,} \\ 7.6^{+0.7}_{-0.5}(\mu)^{+2.8}_{-2.6}(F_0) \pm 0.3(\gamma)^{+2.3}_{-1.4}(\bar{m}_s) & \text{in mSUGRA,} \end{cases} \tag{60}$$

where the second and fourth error are induced by the uncertainties $F_0^{B\to\pi} = 0.28 \pm 0.05$, $F_0^{B\to K} = 0.34 \pm 0.05$, and $\overline{m}_s(2\ \text{Gev}) = (105 \pm 20)$ Mev.

Figure 3 shows the γ dependence of the branching ratios for four $B \to K\pi$ decays. The dots and dashed curves correspond to the central values of the theoretical prediction in the SM and mSUGRA model, respectively. The horizontal slashed bands show the data as given in Table IV.

From Fig. 3 and the numerical results as given in Eqs. (57)–(60), one can see that the SUSY contributions can provide ~50% enhancement to the corresponding branching ratios, and such enhancements can improve the consistency between the theoretical predictions and the data effectively. The central values of the theoretical predictions for $Br(B \to K\pi)$ in the mSUGRA model become well consistent with the experimental measurements.

As for the ratio R_n and R_c as defined in Sec. I, the SM relation $R_c \approx R_n$ remain unchanged in the mSUGRA model. The central values of these two ratios are:

$$R_c^{\rm SM} = 1.17, \quad R_c^{\rm mSUGRA} = 1.15, \tag{61}$$

$$R_n^{\rm SM} = 1.20, \quad R_n^{\rm mSUGRA} = 1.16. \tag{62}$$

The reason is that the SUSY contributions to the four $B \to K\pi$ decays are similar in nature, and thus canceled in the ratio of the corresponding branching ratios.

E. $B \to K\eta^{(\prime)}$ decays

The unexpectedly large branching ratios of $Br(B^\pm \to K^\pm\eta')$ and $Br(B^0 \to K^0\eta')$ were reported by CLEO, *BABAR* and Belle Collaborations[3–5,9], and have been studied in the SM [6] and new physics models by many authors [7,14].

For the branching ratios of $B \to K^\pm\eta'$ and $K^0\eta'$ decays, as can be seen from Tables IV and V, the experimental measurements are about twice that of the central values of the SM predictions in QCD factorization. In the mSUGRA model the SUSY contributions can provide an additional ~30% enhancements, which play an important rule in interpreting the $\eta'K$ puzzle. If we also consider the effects of those dominant errors, the theoretical predictions (in unit of 10^{-6}) are

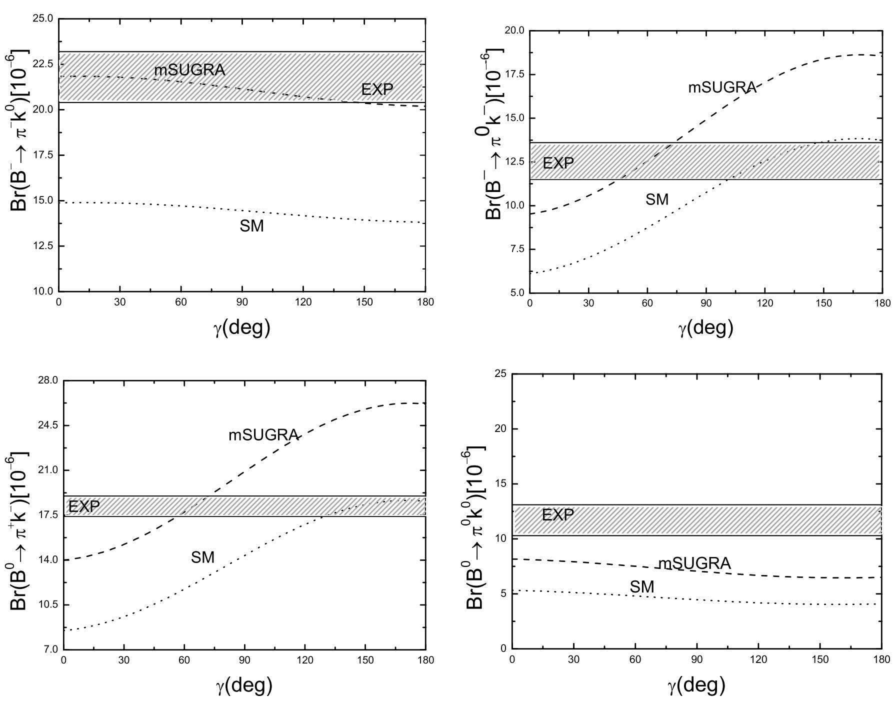

FIG. 3. The γ dependence of the branching ratios of the four $B \to K\pi$ decays in the SM and minimal SUGRA model. The dots and solid curves show the central values of the SM and mSUGRA predictions. The horizontal gray bands show the corresponding experimental measurements as given in Table III.

$$Br(B^- \to K^-\eta') = \begin{cases} 38.1^{+9.4}_{-5.2}(\mu)^{+6.6}_{-5.2}(F_0)^{+13.2}_{-7.4}(\overline{m}_s)^{+1.7}_{-1.2}(\gamma) & \text{in SM,} \\ 49.4^{+11.1}_{-6.1}(\mu)^{+9.6}_{-7.6}(F_0)^{+15.7}_{-8.9}(\overline{m}_s)^{+1.9}_{-1.3}(\gamma) & \text{in mSUGRA,} \end{cases} = \begin{cases} 38.1^{+17.6}_{-10.5} & \text{in SM,} \\ 49.4^{+21.6}_{-13.3} & \text{in mSUGRA,} \end{cases} \tag{63}$$

$$Br(B^0 \to K^0\eta') = \begin{cases} 35.4^{+8.9}_{-5.0}(\mu)^{+6.4}_{-5.0}(F_0)^{+11.9}_{-6.7}(\overline{m}_s) \pm 0.3(\gamma) & \text{in SM,} \\ 45.7^{+10.5}_{-5.9}(\mu)^{+9.1}_{-7.3}(F_0)^{+14.1}_{-8.0}(\overline{m}_s) \pm 0.3(\gamma) & \text{in mSUGRA,} \end{cases} = \begin{cases} 35.4^{+16.2}_{-9.7} & \text{in SM,} \\ 45.7^{+19.8}_{-12.3} & \text{in mSUGRA,} \end{cases} \tag{64}$$

where the individual errors are added in quadrature. The relation between $F_0^{B\to\eta^{(\prime)}}$ and $F_0^{B\to\pi}$ have been defined in Ref. [42]. It is evident that the theoretical predictions in the mSUGRA model are consistent with the data within 1 standard deviation.

For $B^- \to K^-\eta$ and $B^0 \to K^0\eta$ decays, the annihilation contributions are less than 2%, while the SUSY enhancements are about 30%. The numerical results (in unit of 10^{-6}) are

$$Br(B^- \to K^-\eta) = \begin{cases} 2.7^{+0.0}_{-0.1}(\mu)^{+1.0}_{-0.9}(F_0)^{+1.1}_{-0.6}(\overline{m}_s)^{+0.4}_{-0.6}(\gamma) & \text{in SM,} \\ 3.6^{+0.0}_{-0.2}(\mu)^{+1.3}_{-1.1}(F_0)^{+1.4}_{-0.8}(\overline{m}_s)^{+0.5}_{-0.7}(\gamma) & \text{in mSUGRA,} \end{cases} \tag{65}$$

$$Br(B^0 \to K^0\eta) = \begin{cases} 2.0^{+0.0}_{-0.1}(\mu)^{+0.7}_{-0.6}(F_0)^{+1.0}_{-0.6}(\overline{m}_s)^{+0.1}_{-0.2}(\gamma) & \text{in SM,} \\ 2.8^{+0.0}_{-0.1}(\mu)^{+1.0}_{-0.8}(F_0)^{+1.2}_{-0.7}(\overline{m}_s) \pm 0.2(\gamma) & \text{in mSUGRA,} \end{cases} \tag{66}$$

The theoretical predictions in both the SM and the mSUGURA model are all consistent with the data within 1 standard deviation. But the consistency between the theoretical predictions and the data is clearly improved by the inclusion of the SUSY contribution.

In Fig. 4, we show the γ dependence of the branching ratios for four $B \to K\eta^{(\prime)}$ decays. The dots and dashed curves correspond to the central values of the theoretical prediction in the SM and mSUGRA model, respectively. The horizontal slashed bands show the data as given in Table IV.

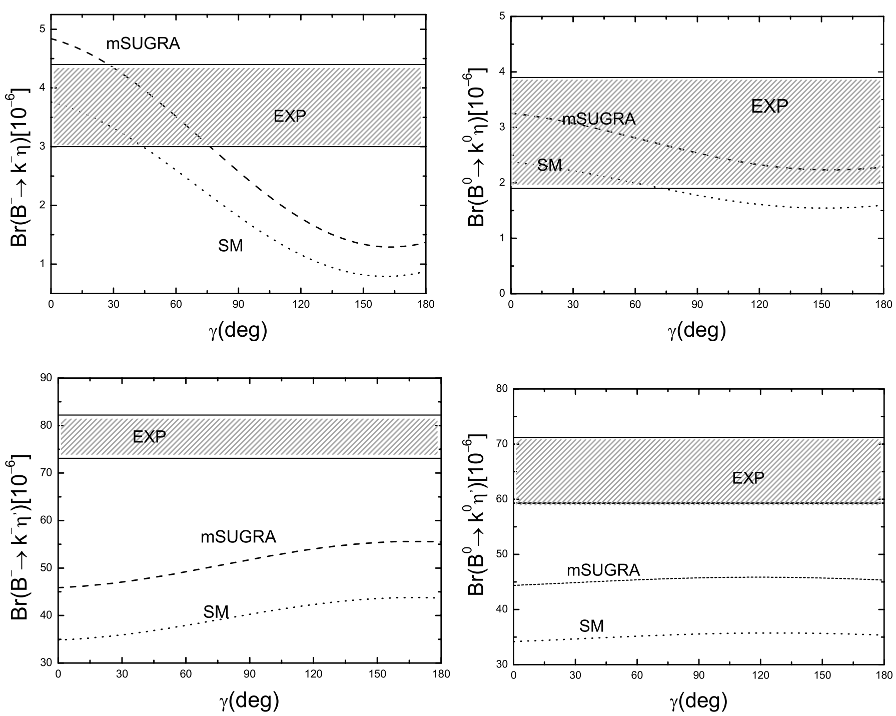

FIG. 4. The γ dependence of the branching ratios $Br(B \to K\eta^{(\prime)})$ in the SM and minimal SUGRA model. The dots and solid curves show the central values of the SM and mSUGRA predictions. The horizontal gray bands show the measured value as given in Table III.

F. $B \to \pi\eta^{(\prime)}$ and $B \to \eta\eta^{(\prime)}$

These seven decay modes are tree-dominated decay processes, and new physics enhancements because the SUSY contributions are less than 10%. For the measured $B^- \to \pi^- \eta$ decay, the theoretical predictions in the SM and the mSUGRA model are

$$Br(B^- \to \pi^- \eta) = \begin{cases} 4.4 + 0.1(\mu)^{+1.4}_{-1.2}(F_0)^{+0.3}_{-0.2}(\overline{m}_s)^{+0.9}_{-1.3}(\gamma) & \text{in SM,} \\ 4.7 + 0.1(\mu)^{+1.5}_{-1.3}(F_0)^{+0.3}_{-0.2}(\overline{m}_s)^{+1.0}_{-1.5}(\gamma) & \text{in mSUGRA,} \end{cases} \tag{67}$$

and consistent with the experimental measurements within 1 standard deviation. For $B^- \to \pi^- \eta'$ decay, the theoretical prediction for its branching ratio is similar to that for $B^- \to \pi^- \eta$ decay, and may be observed soon by the B-factory experiments.

For $B^0 \to \pi^0 \eta^{(\prime)}$ and $B^0 \to \eta^{(\prime)}\eta^{(\prime)}$ decays, the theoretical predictions in the SM and the mSUGRA model are of the order 10^{-7} and smaller than the experimental upper limits.

For B meson decays involving a η or η' as at least one of the two final states, some specific contributions such as the color singlet contribution have been discussed in [47]. These contributions will be in favor of accounting for the experimental data. However, large uncertainties go with them. In our calculations, such contributions are not taken into account.

G. $B \to KK$ decays

For the three $B \to KK$ decay modes, only experimental upper limits are available now. The $B^0 \to K^+K^-$ decay receives only the weak annihilation contribution. Its branching ratio is strongly suppressed in the QCD factorization approach. In Ref. [48], the authors calculate this decay mode by employing the PQCD approach and they also found a small branching ratio. From this decay mode, we can obtain useful information about the long-distance final-state interaction and soft annihilations when the precise experimental measurement becomes available in the future.

For $B^0 \to K^0\overline{K}^0$ and $B^\pm \to K^\pm K^0$ decays, they are penguin-dominant and the SUSY contributions can provide $\sim$20% enhancements to their branching ratios, and still within the experimental upper limits.

H. Uncertainties of theoretical predictions

From the numerical results as given in Table V and in Eqs. (54)–(67), one can see that the theoretical predictions still have large uncertainties.

For most $B \to PP$ decays, the dominant error comes from the uncertainties of the corresponding form factors, since the branching ratios are generally proportional to the square of the related form factors. The measured $Br(B^0 \to \pi^+\pi^-) = (4.6 \pm 0.4) \times 10^{-6}$ prefers a smaller $F_0^{B\to\pi}(0)$, but the large decay rates for $B^0 \to \pi^0\pi^0$ need a large $F_0^{B\to\pi}(0)$. The measured large branching ratios for $B \to K\pi$ and $K\eta'$ decays also favor large $F_0^{B\to K}(0)$ and $F_0^{B\to\eta'}(0)$. Further reduction of the uncertainties of the form factors is essential for us to find the signal of new physics from the $B \to PP$ decays.

The large uncertainty of the light quark masses is also a major source of the theoretical errors. For $B^- \to K^-\eta'$, for example, a 44% enhancement can be obtained by varying $\overline{m}_s$(2 GeV) from 105 MeV to 80 MeV.

The CKM angle γ has a wide scope and can bring large uncertainties to the theoretical predictions for some $B \to PP$ decays in both the SM and the mSUGRA model. Of course, one can also constrain the angle γ from the experimental measurements of $B \to K\pi$ decays [49].

The γ dependence of the branching ratios for those measured $B \to PP$ decays is illustrated in Figs. 2–4. In these figures, the dots and dashed line show the SM and the mSUGRA predictions, respectively. The theoretical uncertainties are not explicitly shown here.

From Figs. 2–4, one can see that some decay modes ($B \to \pi^+\pi^-$, π^0K^-, π^+K^-, etc.) are sensitive to the angle γ in both the SM and the minimal SUGRA model, while other decays such as $B \to \pi^-K^0$, π^0K^0, and $K\eta'$ have a weak dependence on the angle γ. By analyzing the expressions of the decay amplitudes, we find that if the term proportional to V_{ub} is dominant over other terms in the total decay amplitude of a given decay, the branching ratio of this decay will have a strong dependence on the angle γ.

The endpoint divergence of X_H in the hard spectator scattering can produce large uncertainty to the theoretical calculations. But it is generally not important for those tree- or penguin-dominated decay processes because of the strong suppression of the α_s and N_c.

In the QCD factorization approach, the annihilation contributions cannot be calculated reliably, but estimated with large uncertainty. For $B \to PP$ decays, the annihilation contribution may be strongly power-suppressed as discussed by Ali *et al.* [23]. Of course, such assumption has given rise to some controversy.

Finally, when considering the branching ratios in the minimal SUGRA model, different numerical results can be obtained by varying the SUSY parameters $[m_0, m_{1/2}, \tan\beta, A_0, \mathrm{sgn}(\mu)]$ around the given values as listed in Table II. In this paper, we considered two typical sets of SUSY parameters which are still allowed by the data of $B \to X_s\gamma$ and other measurements. In Case A the SUSY contribution is small and can hardly change the SM predictions. On the contrary, in Case B the SUSY contribution is significant in size and provides favorable enhancements to the branching ratios of the penguin-dominant decay modes.

V. SUMMARY

In this paper, we calculated the SUSY contributions to the branching ratios of $B \to PP$ decays in the framework of the mSUGRA model by employing the QCD factorization approach.

In Sec. II , a brief review about the mSUGRA model was given. In Sec. III, we evaluated analytically the new penguin diagrams induced by new particles (gluinos, charged-Higgs bosons, charginos, and neutralinos), and obtained the analytical expressions of the SUSY contributions to the Wilson coefficients. The calculation of $B \to PP$ decays in the QCD factorization approach is also discussed in this section. For the mSUGRA model with the mixing matrix as given in Eq. (28), we found that (a) the SUSY corrections to the Wilson coefficients C_k ($k = 3 - 6$) are very small and can be neglected safely; (b) he leading order SUSY contributions to the Wilson coefficients $C_{7\gamma}(M_W)$ and $C_{8g}(M_W)$ can be rather large, and even change the sign of the corresponding coefficients in the SM.

In Sec. IV, we calculated the branching ratios for 21 $B \to PP$ decays in the SM and the mSUGRA model, and made phenomenological analysis for some well-measured decay modes. From the numerical results, we find the following general features about the new physics effects on the exclusive charmless hadronic $B \to PP$ decays studied in this paper:

(i) For those tree-dominated decays, such as $B \to \pi\pi$, the possible SUSY contributions in the mSUGRA model are very small and can be neglected safely.
(ii) For those penguin-dominated decay modes, the SUSY contributions to their branching ratios can be significant, around 30%-50%.
(iii) For the four $B \to K\pi$ decays, the SUSY contributions to the branching ratios play an important role in improving the consistency of the theoretical predictions with the data.
(iv) For $B \to K\eta'$ decays, the theoretical predictions for branching ratios become consistent with the measured values within 1 standard deviation after the inclusion of the large SUSY contributions in the mSUGRA model. This is a possible interpretation for the so-called $K\eta'$ puzzle.
(v) The theoretical predictions in both the SM and the mSUGRA model still have large theoretical uncertainties. The dominant errors are induced by the uncertainties of the form factors $F_0^{B\to P}$, strange quark mass $\overline{m}_s$, the low-energy scale $\mu \sim m_b$, and the CKM angle γ.

ACKNOWLEDGMENTS

We are very grateful to Cai-dian Lü, Li-bo Guo, Chao-shang Huang, Xiao-hong Wu, Li-gang Jin, and Ying Li for helpful discussions. This work is partially supported by the National Natural Science Foundation of China under Grant No. 10275035, and by the Research Foundation of Nanjing Normal University under Grant No. 214080A916.

APPENDIX: ONE-LOOP FUNCTION AND THE COUPLING CONSTANTS

In this Appendix, the explicit expressions of $f_i(x)$ functions and the coupling constants appeared in Eq. (16)–(23) are presented. For more details, one can see Ref. [34] and references therein.

$$f_1(x) = \frac{1}{12(x-1)^4}(x^3 - 6x^2 + 3x + 2 + 6x\ln x), \quad \text{(A1)}$$

$$f_2(x) = \frac{1}{12(x-1)^4}(2x^3 + 3x^2 - 6x + 1 - 6x^2\ln x), \quad \text{(A2)}$$

$$f_3(x) = \frac{1}{2(x-1)^3}(x^2 - 4x + 3 + 2\ln x), \quad \text{(A3)}$$

$$f_4(x) = \frac{1}{2(x-1)^3}(x^2 - 1 - 2x\ln x), \quad \text{(A4)}$$

$$f_5(x) = \frac{1}{36(x-1)^4}(7x^3 - 36x^2 + 45x - 16 - 12\ln x + 18x\ln x), \quad \text{(A5)}$$

$$f_6(x) = \frac{1}{54(x-1)^4}(37 - 171x + 207x^2 - 73x^3 + 3\ln x - 81x^2\ln x + 54x^3\ln x), \quad \text{(A6)}$$

$$f_7(x) = \frac{1}{18(x-1)^4}(-11x^3 + 18x^2 - 9x + 2 + 6x^3\ln x). \quad \text{(A7)}$$

For the coupling constants $\Gamma^d_{G(LR)}$, $\Gamma^d_{C(LR)}$, $\Gamma^d_{N(LR)}$, we have

$$(\Gamma^d_{GL})^j_I = (\Gamma^D)^j_I, \quad \text{(A8)}$$

$$(\Gamma^d_{GR})^j_I = -(\Gamma^D)^{j+3}_I, \quad \text{(A9)}$$

$$(\Gamma^d_{CL})^{\alpha j}_I = \left[V_1^{*\alpha}(\Gamma^U)^k_I - V_2^{*\alpha}(\Gamma^U)^{k+3}_I \frac{m^u_k}{\sqrt{2}m_W \sin\beta}\right]K_{kj}, \quad \text{(A10)}$$

$$(\Gamma_{CR}^d)_I^{\alpha j} = -U_2^{\alpha}(\Gamma^U)_I^k \frac{m_k^d}{\sqrt{2} m_W \cos\beta} K_{kj}, \tag{A11}$$

$$(\Gamma_{NL}^d)_I^{\alpha j} = \frac{1}{\sqrt{2}}\left[\left(-N_2^{*\alpha} + \frac{1}{3}\tan\theta_W N_1^{*\alpha}\right)(\Gamma^D)_I^j + N_3^{*\alpha}(\Gamma^D)_I^{j+3}\frac{m_j^d}{m_W\cos\beta}\right], \tag{A12}$$

$$(\Gamma_{NR}^d)_I^{\alpha j} = \frac{1}{\sqrt{2}}\left[\frac{2}{3}\tan\theta_W N_1^{\alpha}(\Gamma^D)_I^{j+3} + N_3^{\alpha}(\Gamma^D)_I^j \times \frac{m_j^d}{m_W\cos\beta}\right], \tag{A13}$$

where the K is the CKM matrix.

[1] BaBar Collaboration, edited by P. F. Harrison and H. R. Quinn, Report No. SLAC-R-504, 1998.
[2] T. Hurth, Rev. Mod. Phys. **75**, 1159 (2003); A. J. Buras, R. Fleischer, S. Recksiegel, and F. Schwab, Phys. Rev. Lett. **92**, 101804 (2004); Eur. Phys. J. C **32**, 45 (2003); hep-ph/0402112.
[3] CLEO Collaboration, S. J. Richichi *et al.*, Phys. Rev. Lett. **85**, 520 (2000); CLEO Collaboration, D. Cronin-Hennessy *et al.*, Phys. Rev. Lett. **85**, 515 (2000); CLEO Collaboration, A. Bornheim *et al.*, Phys. Rev. D **68**, 052002 (2003).
[4] *BABAR* Collaboration, B. Aubert *et al.*, Phys. Rev. Lett. **87**, 151802 (2001); **87**, 221802 (2001); **91**, 021801(2003); **91**, 161801 (2003); **91**, 241801 (2003).
[5] Belle Collaboration, K. Abe *et al.*, Phys. Rev. Lett. **87**, 101801 (2001); Phys. Lett. B **517**, 309 (2001); Phys. Rev. Lett. **93**, 021601 (2004); Belle Collaboration, S. H. Lee *et al.*, Phys. Rev. Lett. **91**, 261801 (2003); Belle Collaboration, Y. Chao *et al.*, Phys. Rev. D **69**, 111101 (2004).
[6] D. Atwood and A. Soni, Phys. Lett. B **405**, 150 (1997); A. Datta, X.-G. He, and S. Pakvasa, Phys. Lett. B **419**, 369 (1998); W. S. Hou and B. Tseng, Phys. Rev. Lett. **80**, 434 (1998); A. Ali and C. Greub, Phys. Rev. D **57**, 2996 (1998); D. S. Du, C. S. Kim, and Y. D. Yang, Phys. Lett. B **426**, 133 (1998); M. R. Ahmady, E. Kou, and A.Sugamoto, Phys. Rev. D **58**, 014015 (1998); I. Halperin and A. Zhitnitsky, Phys. Rev. Lett. **80**, 438 (1998); M. Z. Yang and Y. D. Yang, Nucl. Phys. **B609**, 469 (2001).
[7] A. L. Kagan and A. Petrov, hep-ph/9707354; G. R. Lu, Z. J. Xiao, H. K. Guo, and L. X. Lü, J. Phys. G **25**, L85 (1999); Z. J. Xiao *et al.*, Mod. Phys. Lett. A **16**, 441 (2001).
[8] M. Gronau and J. L. Rosner, Phys. Lett. B **572**, 43 (2003).
[9] Heavy Flavor Averaging Group, http://www.slac.-stanford.edu/xorg/hfag/
[10] M. Ciuchini and L. Silvestrini, Phys. Rev. Lett. **89**, 231802 (2002); C.W. Chiang and J. L. Rosner, Phys. Rev. D **68**, 014007 (2003); C. S. Huang and S. H. Zhu, Phys. Rev. D **68**, 114020 (2003); J. F. Cheng, C. S. Huang, and X. H. Wu, Phys. Lett. B **585**, 287 (2004) and references therein.
[11] D. London, hep-ph/0405241; A. Datta *et al.*, hep-ph/0406192.
[12] L. Silvestrini, in *XXXIX Rencontres de Moriond Electroweak Interactions and Unified Theories, La Thuile, March 21-28, 2004* (unpublished).
[13] Z. J. Xiao, W. J. Li, L. B. Guo, and G. R. Lu, Eur. Phys. J. C **18**, 681 (2001); Z. J. Xiao, C. D. Lü, and W. J. Huo, Phys. Rev. D **67**, 094021 (2003).
[14] Z. J. Xiao, C. S. Li, and K. T. Chao, Phys. Rev. D **63**, 074005 (2001); Z. J. Xiao, K. T. Chao, and C. S. Li, Phys. Rev. D **65**, 114021 (2002) and references therein.
[15] D. Atwood, L. Reina, and A.Soni, Phys. Rev. D **55**, 3156 (1997); F. M. Borzumati and C. Greub, Phys. Rev. D **58**, 074004 (1998); **59**, 057501 (1999); T. M. Aliev and E. O. Iltan, J. Phys. G **25**, 989 (1999); D. Bowser-Chao, K. Cheung, and W. Y. Keung, Phys. Rev. D **59**, 115006 (1999); Y. B. Dai, C. S. Huang, and H.W. Huang, Phys. Lett. B **390**, 257 (1997); C. S. Huang, W. Liao, Q. S. Yan, and S. H. Zhu, Phys. Rev. D **63**, 114021 (2001); **64**, 059902(E) (2001); J. J. Cao, Z. J. Xiao, and G. R. Lu Phys. Rev. D **64**,014012 (2001); D. Zhang, Z. J. Xiao, and C. S. Li, Phys. Rev. D **64**, 014014 (2001).
[16] H. Baer, M. Brhlik, D. Castaño, and X. Tata, Phys. Rev. D **58**, 015007 (1998); H. Baer and M. Brhlik, Phys. Rev. D **55**, 3201 (1997).
[17] T. Goto, T. Nihei, and Y. Okada, Phys. Rev. D **53**, 5233 (1996); **54**, 5904(E) (1996).
[18] T. Goto, Y. Okada, Y. Shimizu, and M. Tanaka, Phys. Rev. D **55**, 4273 (1997); **66**, 019901(E) (2002).
[19] H. H. Asatryan and H. M. Asatrian, Phys. Lett. B **460**, 148 (1999); A. Ali, P. Ball, L. T. Handoko, and G. Hiller, Phys. Rev. D **61**, 074024 (2000) ;C. Bobeth, A. J. Buras, F. Krüger, and J. Urban, Nucl. Phys. **B630**, 87 (2002) and references therein; C. S. Huang, W. Liao, and Q. S. Yan, Phys. Rev. D **59**, 011701(R) (1999); J. F. Cheng, C. S. Huang, and X. H. Wu, hep-ph/0404055.
[20] A. Djouadi *et al.*, hep-ph/9901246.
[21] R. Barbieri, S. Ferrara, and C. A. Savoy, Phys. Lett. B **119**, 343 (1982); A. H. Chamseddine, R. Arnowitt, and P. Nath, Phys. Rev. Lett. **49**, 970 (1982); L. Hall, J. Lykken, and S. Weinberg, Phys. Rev. D **27**, 2359 (1983).
[22] C.S. Huang and X. H. Wu, Nucl. Phys. **B657**, 304 (2003).
[23] A. Ali, G. Kramer, and Cai-Dian Lü, Phys. Rev. D **58**, 094009 (1998).
[24] Y. H. Chen, H. Y. Cheng, B. Tseng, and K. C. Yang, Phys. Rev. D **60**, 094014 (1999).

[25] M. Beneke, G. Buchalla, M. Neubert, and C. T. Sachrajda, Phys. Rev. Lett. **83**, 1914 (1999); Nucl. Phys. **B591**, 313 (2000).

[26] M. Beneke, G. Buchalla, M. Neubert, and C. T. Sachrajda, Nucl. Phys. **B606**, 245 (2001).

[27] M. Beneke and M. Neubert, Nucl. Phys. **B675**, 333 (2003).

[28] D. S. Du, H. J. Gong, J. F. Sun, D. S. Yang, and G. H. Zhu, Phys. Rev. D **65**, 074001 (2002); D. S. Du, J. F. Sun, D. S. Yang, and G. H. Zhu, Phys. Rev. D **67**, 014023 (2003).

[29] Chia-Hung V. Chang, Hsiang-nan Li, Phys. Rev. D **55**, 5577 (1997); T.-W. Yeh and Hsiang-nan Li, Phys. Rev. D **56**, 1615 (1997); Y.-Y. Keum, Hsiang-nan Li, and A. I. Sanda, Phys. Rev. D **63**, 054008 (2001); Y.-Y. Keum and Hsiang-nan Li, Phys. Rev. D **63**, 074006 (2001); C. D. Lü, K. Ukai, and M. Z. Yang, Phys. Rev. D **63**, 074009 (2001);C. D. Lü and M. Z. Yang, Eur. Phys. J. C **23**, 275 (2002).

[30] S. Mishima and A. I. Sanda, Phys. Rev. D **69**, 054005 (2004).

[31] Particle Data Group, K. Hagiwara *et al.*, Phys. Rev. D **66**, 010001 (2002).

[32] A. Djouadi, J.L. Kneur and G. Moultaka, hep-ph/ 0211331.

[33] C. Bobeth, T. Ewerth, F. Krüger, and J. Urban, Phys. Rev. D **64**, 074014 (2001).

[34] P. Cho, M. Misiak and D. Wyler, Phys. Rev. D **54**, 3329 (1996).

[35] A. J. Buras, in *Probing the Standard Model of Particle Interactions*, edited by F. David and R. Gupta (Elsevier Science B.V., New York, 1998); hep-ph/ 9806471.

[36] M. Kabayashi and T. Maskawa, Prog. Theor. Phys. **49**, 652 (1973).

[37] G. Buchalla, A.J. Buras, and M.E. Lautenbacher, Rev. Mod. Phys. **68**, 1125 (1996).

[38] C. Bobeth, T. Ewerth, F. Krüger, and J. Urban, Phys. Rev. D **66**, 074021 (2002).

[39] S. A. Abel, W. N. Cottingham, and I. B. Whittingham, Phys. Rev. D **58**, 073006 (1998).

[40] W. N. Cottingham, H. Mehrban, and I. B. Whittingham, Phys. Rev. D **60**, 114029 (1999).

[41] M. Bauer and B. Stech, Phys. Lett. B **152**, 380 (1985); M. Bauer, B. Stech, and M. Wirbel, Z. Phys. C **29**, 637 (1985); **34**, 103 (1987).

[42] T. Feldmann, P. Kròll, and B. Stech, Phys. Rev. D **58**, 114006 (1998).

[43] G-C. Cho, K. Hagiwara, Nucl. Phys. **B574**, 623 (2000).

[44] BaBar Collaboration, B. Aubert *et al.*, Phys. Rev. Lett. **92**, 061801 (2004).

[45] S. Laplace, hep-ph/0209188; A. Höcker *et al.*, Eur. Phys. J. C **21**, 225 (2001).

[46] Belle Collabloration, K. Abe, in *Lake Louise Winter Institute 2004, Canada* (unpublished).

[47] M. Beneke and M. Neubert, Nucl. Phys. **B651**, 225 (2003).

[48] C. H. Chen and Hsiang-nan Li, Phys. Rev. D **63**, 014003 (2001).

[49] Z. J. Xiao and M. P. Zhang, Phys. Rev. D **65**, 114017 (2002) and reference therein.